Environmental Pollution 357 (2024) 124387

Contents lists available at ScienceDirect

Environmental Pollution

journal homepage: www.elsevier.com/locate/envpol

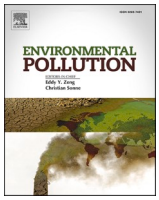

Chronological distribution and potential sources of persistent toxic substances in soils from the glacier foreland of Midtre Lovénbreen, Svalbard☆

Jihyun Cha [a], Jung-Hyun Kim [b], Ji Young Jung [c], Seung-Il Nam [b], Seongjin Hong [a,d,*]

[a] Department of Earth, Environmental & Space Sciences, Chungnam National University, Daejeon, 34134, Republic of Korea
[b] Division of Glacier and Earth Sciences, Korea Polar Research Institute, Incheon, 21990, Republic of Korea
[c] Division of Life Sciences, Korea Polar Research Institute, Incheon, 21990, Republic of Korea
[d] Department of Marine Environmental Sciences, Chungnam National University, Daejeon, 34134, Republic of Korea

ARTICLE INFO

Keywords:
Svalbard
Glacier foreland
Soil
Persistent toxic substances
Coal

ABSTRACT

Despite its reputation as one of the cleanest regions globally, recent studies have identified the presence of various persistent toxic substances (PTSs) in the environmental matrices collected from Svalbard. This study investigated the chronological distribution and potential sources of 81 PTSs in soils from the glacier foreland of Midtre Lovénbreen. Soil samples (n = 45) were categorized by age based on exposure to the atmosphere due to glacier retreat in July 2014 into five age groups: 80–100 years (n = 7), 60–80 years (n = 12), 40–60 years (n = 16), 20–40 years (n = 7), and <20 years (n = 3). Concentrations of polychlorinated biphenyls (PCBs, n = 32) in soils varied with age, ranging from 0.29 to 0.74 ng g^{-1} dw. In addition, the concentrations of polycyclic aromatic hydrocarbons (PAHs, n = 28), perylene, and alkyl-PAHs (n = 20) in soils ranged from 21 to 80 ng g^{-1} dw, 2.9–62 ng g^{-1} dw, and 73–420 ng g^{-1} dw, respectively. The concentrations of PTSs were observed to be greater in older soils. Principal component analysis revealed that PCBs in soils originated from various product sources. Positive matrix factorization modeling estimated the association of PAHs in soils with potential origins, such as diesel emissions, petroleum and coal combustion, and coal. Potential sources of PAHs were mainly coal in younger soils and diesel emissions and petroleum combustion in older soils. Alkyl-PAH compositions in the soil were similar to those of bituminous coal, with a noteworthy degree of weathering observed in older soils. The accumulation rate and flux of PTSs in soils exhibited compound-specific patterns, reflecting factors such as long-range transport, fate, origin, and recent inputs. These findings can serve as baseline data for protecting and preserving polar environments.

1. Introduction

The Earth's climate system is experiencing profound impacts due to climate change, characterized by a continuous increase in the global average temperature associated with elevated CO_2 concentrations in the atmosphere (Lynas et al., 2021). This phenomenon leads to various climate anomalies such as droughts, floods, cold spells, desertification, and disruptions in ecosystems worldwide (Schellnhuber et al., 2016). The Arctic region is particularly susceptible to significant and potentially irreversible transformations induced by climate change (Schellnhuber et al., 2016). Over the past five decades, the average temperature in the Arctic has increased by almost four times the global average, resulting in glacial retreat, permafrost thawing, and sea-ice reduction (Rantanen et al., 2022). These rapid environmental changes profoundly impact the Arctic ecosystem (Venkatachalam et al., 2021).

Svalbard, an archipelago at the gateway from the North Atlantic to the Arctic, consists of nine islands, with approximately 57% of the land covered by glaciers (Miner et al., 2021; Nuth et al., 2013). The diverse environmental compartments of Svalbard provide a conducive environment for unique, region-specific, long-term biological, and chemical reservoirs (Miner et al., 2021). Despite being considered one of the most pristine regions globally, Svalbard has exhibited traces of various

☆ This paper has been recommended for acceptance by Charles Wong.

* Corresponding author. Department of Marine Environmental Sciences, Chungnam National University, 99 Daehak-ro, Yuseong-gu, Daejeon, 34134, Republic of Korea.
E-mail address: hongseongjin@cnu.ac.kr (S. Hong).

https://doi.org/10.1016/j.envpol.2024.124387
Received 8 April 2024; Received in revised form 11 June 2024; Accepted 16 June 2024
Available online 17 June 2024

persistent toxic substances (PTSs) in environmental samples over the past three decades (Miner et al., 2021). Common PTSs include polychlorinated biphenyls (PCBs) and polycyclic aromatic hydrocarbons (PAHs). PCBs have been utilized across industries since 1929 because of their distinctive insulating and flame-retardant properties (Aslam et al., 2019). They have been incorporated into insulating oil for transformers, circuit breakers, and electronic devices (Kim et al., 2021). PAHs originate from anthropogenic sources, such as incomplete combustion of petroleum, vehicle exhaust, waste incineration, food preparation, and metal smelting (Na et al., 2021). Additionally, PAHs can be generated from natural sources, such as volcanic eruptions, forest fires, and biomass burning (Wilcke, 2007). These compounds can accumulate in environmental media, such as soil and sediment, and are known to have adverse effects on terrestrial and marine organisms (Kim et al., 2021). PTSs introduced into high-latitude areas may not readily evaporate due to low temperatures and preferential precipitation, potentially accumulating in the Arctic regions (Wania and Westgate, 2008).

The Midtre Lovénbreen is located in Svalbard and has experienced a rapid glacial retreat in recent years due to increasing temperatures (Ai et al., 2019). The glacier foreland became newly exposed to the atmospheric environment as the glaciers receded. This gradual glacial retreat transformed the foreland into an ideal site for observing changes in organic matter over time (Eichel et al., 2015; Khedim et al., 2021). Consequently, the surrounding environment has undergone significant transformation, underscoring the importance of monitoring and understanding environmental changes in this area (Schellnhuber et al., 2016). Glacio-fluvial runoff resulting from glacier retreat can alter the biogeochemical properties of soils, vegetation composition, and grain size distribution (Kim et al., 2022). Soil is a repository of various environmental pollutants that accumulate upon exposure to the atmosphere (Birks et al., 2017; Casal et al., 2018). Previous studies have highlighted the significance of soil as a crucial environmental medium for the accumulation of PAHs, constituting more than 90% of the total environmental load (Aichner et al., 2015; Qu et al., 2020). Arctic soil, which is often frozen year-round, restricts nutrient movement and slows chemical reactions, leading to nutrient deficiency, whereas sparse vegetation contributes to the slow decomposition of organic matter (Wild et al., 2014). Recent studies have found that global warming and other disturbances release PTSs stored in Arctic soils (Cabrerizo et al., 2018).

As the Arctic undergoes unprecedented warming and glacier retreat, these changes significantly affect the distribution and accumulation of PTSs in the soil. However, few studies have been conducted on the chronological distribution of PTS in soils exposed to the atmosphere following glacial retreat. This study hypothesized that the distribution and potential sources of PTSs in soils are influenced by soil age, glacio-fluvial runoff, human activities, and buried materials of natural origin. The primary objective of this study was to investigate the chronological distribution of PTSs in soils from the Midtre Lovénbreen glacier foreland of Svalbard after the glacier retreat. We compared PTS concentrations in soils at sites affected and unaffected by glacio-fluvial runoff. Potential sources of PTSs were estimated using statistical analysis, multivariate modeling, and composition ratios of individual compounds in the soils. In addition, this study assessed the accumulation rate and flux of PTSs in the soil over the past 100 years. This comprehensive approach could provide insights into the mechanisms and characteristics of PTS accumulation in Arctic soils and potentially contribute to protecting the health of terrestrial ecosystems vulnerable to pollution.

2. Materials and methods

2.1. Study area and sample collection

Arctic Svalbard encompasses both discontinued and active mining areas (Fig. 1a). The Midtre Lovénbreen glacier foreland is situated on the Brøggerhalvøya peninsula in the western part of Spitsbergen (Fig. 1b). In July 2014, 45 soil samples (0–5 cm) were collected from the Midtre Lovénbreen glacier foreland, representing various soil ages exposed to

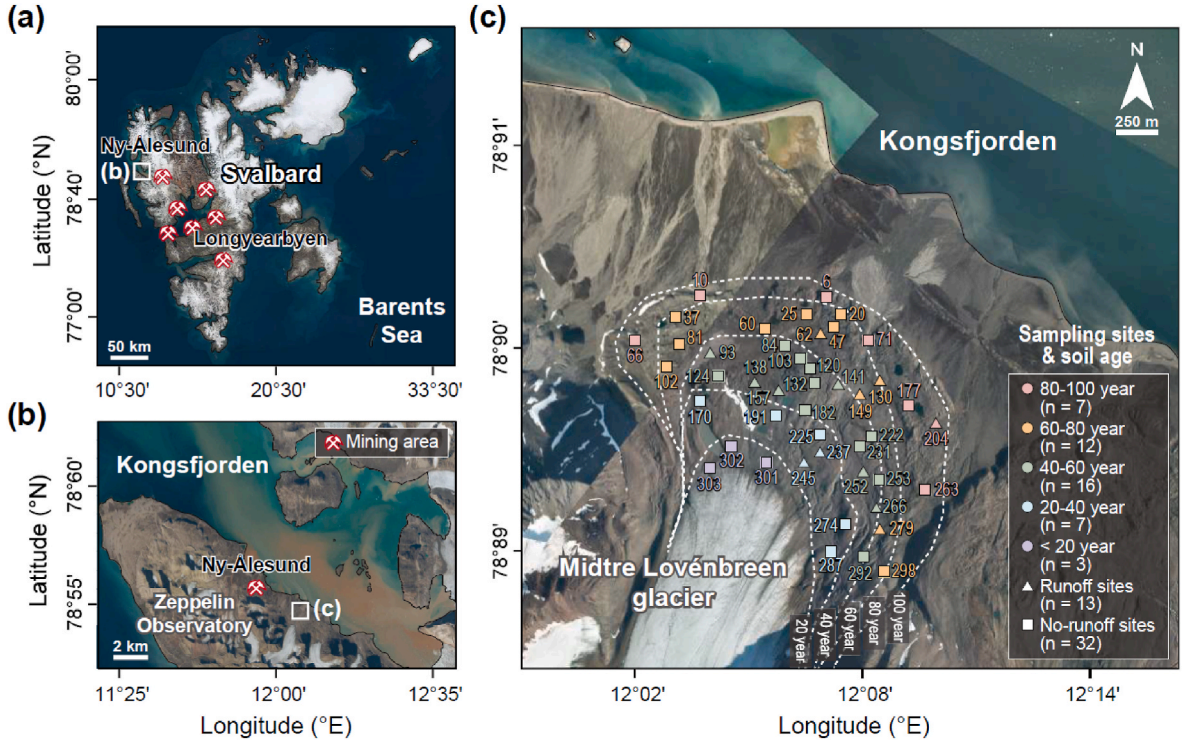

Fig. 1. Map showing the sampling sites in **(a)** the Arctic Svalbard, **(b)** Ny-Ålesund, and **(c)** Midtre Lovénbreen. Forty-five soil samples (0–5 cm) were collected from the foreland of the Midtre Lovénbreen glacier in July 2014. The white lines indicate the glacier retreat timeline as of 2014. Triangles and squares represent sites affected and unaffected by glacio-fluvial runoff, respectively.

the atmosphere due to glacier retreat (Fig. 1c and Table S1). Detailed information regarding the sampling sites and labeling of soil samples has been provided in previous studies (Kim et al., 2022; Moreau et al., 2005). Soil age was categorized into five intervals: 80–100 years (n = 7), 60–80 years (n = 12), 40–60 years (n = 16), 20–40 years (n = 7), and less than 20 years (n = 3). The sampling sites were divided into sites affected by glacio-fluvial runoff (runoff sites; n = 13) and sites not affected by it (no-runoff sites; n = 32) (Kim et al., 2022; Moreau et al., 2005). Soil samples were air-dried, passed through a 2 mm sieve, and homogenized. Soil organic carbon (SOC), total nitrogen (TN), and grain size distribution were analyzed and partially reported in a previous study (Kim et al., 2022).

2.2. PTSs analysis in soils

A total of 81 PTSs were analyzed in the soils, including 32 PCBs, 29 PAHs (including perylene), and 20 alkyl-PAHs (Table S2). Thirty-two PCBs were obtained from Wellington Laboratories (Guelph, ON, Canada). Twenty-nine PAHs were obtained from ChemService (West Chester, PA) and Sigma-Aldrich (St. Louis, MO). Twenty alkyl-PAHs were purchased from Wellington Laboratories. Five grams of soil were placed in a stainless steel cell and subjected to extraction with dichloromethane (DCM, Honeywell, Charlotte, NC) using an accelerated solvent extractor (Dionex ASE 350, Thermo Scientific, Salt Lake, UT). During the experimental procedures, blank samples were analyzed alongside soil samples to detect any potential contamination by the target compounds. Before organic extraction, mass-labeled surrogate standards were added for quality control (Table S2). Extraction was performed for 20 min at 120 °C, and the extract was collected in a 60 mL glass vial and concentrated to 1 mL using gentle N_2 gas. The organic extract was reacted with activated copper powder (Sigma-Aldrich) for approximately 1 h to eliminate elemental sulfur. The extract was separated and purified using open-column silica gel chromatography (8 g; Sigma-Aldrich). Eight grams of activated silica gel, infused with hexane were packed into a glass column. The first fraction for PCB analysis was eluted with 30 mL hexane (Honeywell). The second fraction for the analysis of PAHs and alkyl-PAHs was eluted with 60 mL hexane:DCM (8:2, v:v).

The concentrations of PCBs, PAHs, and alkyl-PAHs were measured using an Agilent 7890B gas chromatograph (GC) coupled with a 5977B mass selective detector (MSD, Agilent Technologies, Santa Clara, CA). The instrument conditions for GC-MSD are listed in Table S3. A DB-5MS column was used for compound separation. Due to the limited availability of pure standards for each alkyl-PAH, the concentrations of each methyl substituent of the PAHs were semiquantified using 20 model compounds (Hong et al., 2012). The quantification ion, confirmation ion, method detection limit, and recoveries of the individual compounds are presented in Table S2.

2.3. qGIS mapping

In this study, the Quantum Geographical Information System software (qGIS, Version 3.28.3) was used to establish the spatial distribution of PTSs in soils. qGIS software enables the visualization and analysis of the distribution of PTSs in a specific region. The basemap layer for Svalbard was obtained from the Norwegian Polar Research Institute (https://geodata.npolar.no/). The layers of the cached basemap were selected from Svalbard Orthophoto.

2.4. Principal component analysis

Principal component analysis (PCA) was conducted using IBM SPSS Statistics 26 (SPSS Inc., Chicago, IL) to identify potential sources of PCBs in soils. Bartlett's and Kaiser-Meyer-Olkin (KMO) tests were performed to evaluate the suitability of the data for statistical analysis. In this study, the KMO value exceeded the guideline value of 0.6, confirming the suitability of the dataset for PCA. PCA utilized the relative proportions of seven types of PCB homologs, corresponding to products and combustion origins, as described in a previous study (Pedersen et al., 2015).

2.5. Positive matrix factorization modeling

The United States Environmental Protection Agency (EPA) positive matrix factorization (PMF) multivariate modeling (Version 5.0) was used to identify potential sources of PAHs in soils. The PMF model, which is employed to trace the sources of toxic substances, utilizes a mathematical algorithm to convert negative values resulting from factor analysis into positive values (Kim et al., 2021). This process yields the least squares value for each dataset (Moon et al., 2008). PAHs utilized for PMF modeling included EPA 15 priority PAHs excluding naphthalene (Na) (Lee et al., 2023). The input datasets comprised 15 PAHs across 45 sites. During the analysis of the PMF model, it is imperative to minimize the Q_{True}/Q_{Exp} ratio when determining the number of factors representing pollutant sources. In this study, four factors were confirmed to have the smallest value of Q_{True}/Q_{Exp}. Thus, factors for potential sources were estimated based on the '% of species' of individual compounds (Kim et al., 2021). The foundational models underwent 100 iterations and linear regression analysis revealed a coefficient of 0.99 (R^2) between the predicted and estimated concentrations, indicating a satisfactory performance of the PMF model results.

2.6. Estimations for accumulation rate and flux of PTSs

The present study determined the accumulation rate and flux of PTSs in the soil. The calculation of the accumulation rate of PTSs in soils was slightly modified from the method used in a previous study (Fang et al., 2017). The accumulation rate was computed by dividing the average age of each soil age group by the concentration of PTSs in the soils. For example, the mean ages for the age groups 80–100 years, 60–80 years, 40–60 years, 20–40 years, and <20 years were calculated as 84, 68, 51, 32, and 7 years, respectively. Additionally, the accumulation flux of PTSs in the soils was calculated using the difference in age for each soil group. For instance, the accumulation flux for 1926–1934 was derived from the PTS concentrations in soils for the age group of 80–100 years minus that for the age groups of 60–80 years.

2.7. Data collection for PTSs in air samples in Svalbard

All data on PCBs and PAHs in the air samples were collected from the EBAS database of the Norwegian Institute for Air Research (http://ebas.nilu.no/). The concentrations of PCBs and PAHs in air samples were measured at the Zeppelin Observatory from Svalbard in 1998 and 1994, respectively. The Zeppelin Observatory, operated by the Norwegian Polar Research Institute, is a research station located at Ny-Ålesund on the Spitsbergen-Svalbard archipelago (Fig. 1b). The study area was approximately 3 km from the observatory. Changes in the concentrations of PCBs and PAHs according to soil age were compared with trends in the concentrations of PTSs in the air samples.

3. Results and discussion

3.1. Distributions of PCBs, PAHs, and alkyl-PAHs in soils

Detailed information on soil characteristics, such as SOC, TN, and grain size distribution, is presented in the Supplementary Text (Fig. S1 and Table S1). Concentrations of 32 PCBs in soils varied with age, ranging from 0.29 ± 0.03 to 0.74 ± 0.19 ng g^{-1} dw (Fig. 2a and Table S4). Significant differences in PCB concentrations were observed between soils aged 80–100 years and those aged 20–40 years, as well as soils less than 20 years old, indicating a notable decreasing trend in PCB concentrations. These declining trends in PCB concentrations are likely attributed to global regulations governing their production and use since

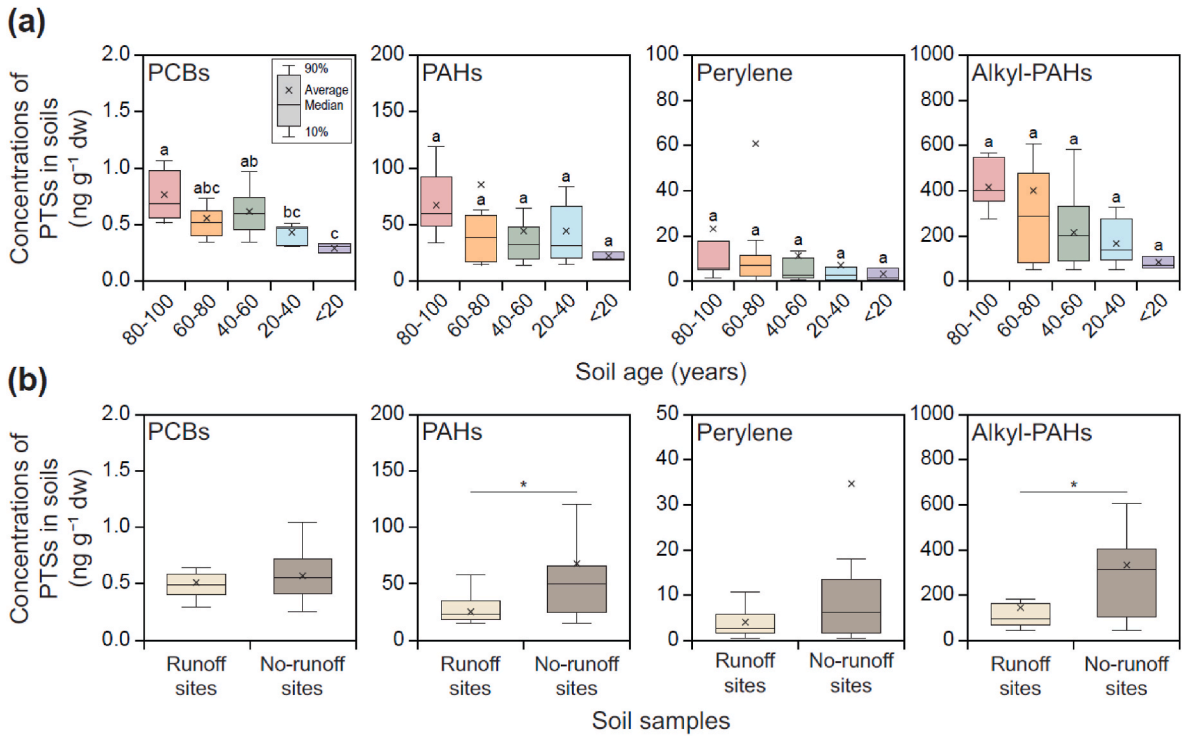

Fig. 2. (a) Concentrations of PCBs, PAHs, perylene, and alkyl-PAHs in soil samples categorized by soil age. Different letters based on the Kruskal-Wallis test indicate significant differences ($p < 0.05$) in the concentrations of PTSs between soil ages. **(b)** Concentrations of PTSs in soils of runoff sites and no-runoff sites from the glacier foreland of Midtre Lovénbreen, Svalbard. The asterisk (*) indicates statistically significant differences in the concentrations of PTSs between the soil samples ($p < 0.05$, Welch's *t*-test).

the 1970s (Aslam et al., 2019; Zhang et al., 2014a). Thus, the observed decreases in PCB concentrations reflect consistent global efforts to mitigate the impact of these pollutants on Arctic ecosystems (Ma et al., 2016). The concentration of PCBs in soils showed comparability between runoff sites (0.5 ng g^{-1} dw) and no-runoff sites (0.6 ng g^{-1} dw) (Fig. 2b). This suggests that PCBs in soils are resistant to washing away by glacio-fluvial runoff, likely due to their strong adsorption to soils and hydrophobic properties (Liu et al., 2015). Although older soils may have been influenced by glacio-fluvial runoff during the initial decades of their formation, the classification of runoff and no-runoff sites was based on a specific timeframe (Kim et al., 2022; Moreau et al., 2005). A positive correlation between PCB concentrations and SOC contents was observed (Fig. S2), which is consistent with the findings of a previous study (Zhang et al., 2014a). The spatial distribution of PCBs in soils showed high concentrations at ML204 (1.1 ng g^{-1} dw), ML102 (1.1 ng g^{-1} dw), and ML6 (0.97 ng g^{-1} dw) (Fig. S3). Notably, ML102 (0.83%) exhibited high SOC content, whereas ML204 and ML6 had SOC contents of 0.33% and 0.19%, respectively, which were lower than the average SOC content in this area.

The concentrations of 28 PAHs in soils exhibited variations based on soil age, ranging from 21 ± 1.8 to 80 ± 150 ng g^{-1} dw (Fig. 2a and Table S5). Although the concentration of PAHs was higher in the older soils, no significant differences were observed. Recently, despite a global decrease in PAH emissions, temporal trends in PAHs measured within various Arctic media have not shown a decreasing trend (Yu et al., 2019). This may be due to the influence of anthropogenic activities such as resource exploration, scientific research, and tourism in the Arctic regions (Na et al., 2021). The concentration of PAHs in the soils showed a positive correlation with SOC content (Fig. S2), suggesting that older soils have higher SOC content due to the influence of vegetation, and that the concentration of PAHs is also high in sites with high SOC content. The concentration of PAHs in soils at the no-runoff sites was approximately 2.5 times higher than that at runoff sites, indicating a potential impact of glacio-fluvial runoff on the fate of PAHs in soils (Fig. 2b). This trend showed a somewhat different pattern from the results for PCBs in the soils. These variations can be attributed to differences in the chemical properties, sorption behaviors, and transport pathways of PCBs and PAHs (Liu et al., 2015). The highest concentrations of PAHs in soils were found at ML102 (570 ng g^{-1} dw) and ML222 (200 ng g^{-1} dw) (Fig. S3). Among PAHs in soils, phenanthrene (Phe) showed the highest average concentration (21 ng g^{-1} dw), followed by fluorene (Flu; 4.7 ng g^{-1} dw). Phe originates from both natural and anthropogenic sources. For example, Phe in soil can biologically originate from alkyl phenanthrene precursors in plant debris (Sims and Overcash, 1983). Previous studies have reported significant peaks of Phe, an indicator of PAH contamination from coal, in abandoned coal samples from the Ny-Ålesund, indicating substantial PAH contamination from coal sources (Howaniec et al., 2018; Steenhuisen and van den Heuvel-Greve, 2021). Additionally, Flu is commonly recognized as an indicator of potential contamination associated with coal in environmental samples (Howaniec et al., 2018).

The concentrations of perylene in soils ranged from 2.9 ± 2.0 to 62 ± 180 ng g^{-1} dw across different age categories, with no significant differences observed (Fig. 2a and Table S5). There were also no significant differences in the perylene concentrations between the runoff and no-runoff sites (Fig. 2b). The soils collected from ML102 and ML177 exhibited the highest concentrations of perylene at 670 ng g^{-1} dw and 110 ng g^{-1} dw, respectively (Fig. S3). The perylene concentration in the soil did not show a significant relationship with SOC (Fig. S2). Previous studies have indicated that perylene can naturally occur at low temperatures and may also be partially generated during combustion (Gocht et al., 2007; Opuene et al., 2007; Zhang et al., 2014b). In addition, it has been reported that the chemical structure and high concentrations of lignin-derived aromatic compounds produced by fungi and plants in soils are related to the formation of perylene precursors (Bakhtiari et al., 2010). These factors are expected to contribute to the variation in perylene concentration in the soils of the study area.

The concentrations of the 20 alkyl-PAHs in soils varied across

different age groups, ranging from 73 ± 22 to 420 ± 95 ng g^{-1} dw (Fig. 2a and Table S6). The concentration of alkyl-PAHs in soils did not exhibit significant differences between age groups, suggesting the potential ongoing presence of these compounds. This persistence may be attributed to alkyl-PAHs of coal origin, which are naturally buried in the soils of this region. Additionally, the study area was located 3 km from Ny-Ålesund, where coal mining was actively conducted from 1916 to 1963 (Dowdall et al., 2004). Although mining activities have ceased, there is still the possibility of soil contamination due to the remnants of machinery, equipment, and waste, as well as the dispersion of coal residue and fine coal particles (Kozak et al., 2013). The concentration of alkyl-PAHs in soils exhibited a notable correlation with the SOC content (Fig. S2). In addition, the concentration of alkyl-PAHs at the no-runoff sites was approximately 2.5 times higher than that at the runoff sites (Fig. 2b). Among the sampling sites, ML102 had the highest concentration of alkyl-PAHs at 2000 ng g^{-1} dw, followed by ML47 (600 ng g^{-1} dw), and ML222 (580 ng g^{-1} dw) (Fig. S3). These results indicate that PAHs and alkyl-PAHs in soils have similar distribution patterns and behaviors. Among the sampling sites, ML102 was characterized by the highest clay content (17%) and the third-highest SOC content (0.83%). Previous studies have shown that clay and organic carbon contents in environmental media are positively correlated with the concentrations of organic pollutants (Li et al., 2019; Yang et al., 2010). Additionally, because ML102 was not affected by glacio-fluvial runoff, it was expected that PAHs, perylene, and alkyl-PAHs would not be washed away. Thus, it is believed that ML102 showed elevated concentrations of PAH, perylene, and alkyl-PAHs in the soil due to the influence of these factors. Given that the presence of vegetation in the study area may significantly influence the distribution, production, and transformation of PTSs (Li et al., 2023; Masclet et al., 1987), it is imperative to investigate the relationship between the quantity and type of vegetation and the distribution of PTSs in this region.

3.2. Potential sources of PCBs, PAHs, and alkyl-PAHs

The composition of PCBs in soils predominantly featured tetra-CBs at most sites, indicating the potential influence of long-range transport (Fig. S4). This trend has also been observed in various environmental media in Svalbard, including sediments, vegetation, and soil (Aslam et al., 2019; Lee et al., 2023). This is attributed to the higher volatility of low-chlorinated congeners, which are more suitable for long-range transport (Jiao et al., 2009). Consequently, the cold and remote nature of the Arctic environment makes it particularly vulnerable to the accumulation of low-chlorinated PCBs that travel through the atmosphere. However, the composition of di-CBs and tri-CBs was low at all sites, likely influenced by temperature during sampling (Wania et al., 1998). The effect of glacio-fluvial runoff on PCB composition in the soils was minimal. The PCA results indicated that PCBs mainly originated from product sources, such as Aroclor, Clophen A, and Kanechlor (Fig. 3a), consistent with a previous study suggesting potential sources of PCBs in the Arctic region, such as obsolete equipment containing PCBs (Aslam et al., 2019). In an earlier study, potential sources of PCBs in snow samples from Svalbard were reported to be of product origin (Hermanson et al., 2020), whereas PCBs in sediments were assumed to originate from combustion (Lee et al., 2023). This variation could be attributed to the fate and adsorption properties of PCBs in the environmental medium, as well as the temperature at the time of sampling. Among the PCB congeners, PCB52 exhibited the most significant influence. PCB52 is present in most commercial substances and has been identified as one of the most prevalent congeners in the atmospheric environment of Svalbard (Aslam et al., 2019; Ubl et al., 2017). Conversely, PCB28 showed a negative relationship with soil samples. PCB28 is primarily transported in a gaseous state from mid-latitudes to the Arctic region and is known to persist in a gaseous state in Svalbard (Eckhardt et al., 2007). Its concentration is closely linked to temperature, suggesting potential re-volatilization from the soil to the atmosphere as temperature increases. Thus, PCB28 in soils collected during summer could exist in a gaseous state. These findings suggest that as temperature rises, low-molecular-weight PCBs in Arctic soils may volatilize back into the atmosphere.

The PAHs in the soils predominantly consisted of low-molecular-weight PAHs, especially 3-ring PAHs (Fig. S4). This trend suggests that global distillation driven by long-range transport may predominate (Wania and Mackay, 1996). However, previous studies investigating the origin of PAHs in soils from Svalbard have indicated that although PAHs in this area may be influenced by long-range transport, they are primarily affected by local contamination from mining activities (Marquès et al., 2017; Na et al., 2021). The similarity in PAH composition across all sites suggested minimal influence from glacio-fluvial runoff. Potential sources of PAHs in the soils were assessed using the PMF model. The PMF model results revealed that the sources of PAHs in the soils included diesel emission, petroleum combustion, coal combustion, and coal (Fig. S5). Factor 1 likely originated from diesel emissions because of the predominance of dibenz[*a,h*]anthracene (DbahA) and indeno[*1,2,3-cd*]pyrene (Harrison et al., 1996; Lee et al., 2022). Factor 2 was dominated by benzo[*b*]fluoranthene and benzo[*g,h,i*]perylene (BghiP), and petroleum combustion was identified as a potential source (Lee et al., 2023). Factor 3 was dominated by benzo[*k*]fluoranthene (BkF) and was assumed to originate from coal combustion (Ravindra et al., 2008). Factor 4 was dominated by compounds such as Flu and Phe, which were predicted to be of coal origin (Lee et al., 2023). For soil samples aged 80–100 years, a combination of four factors contributed to

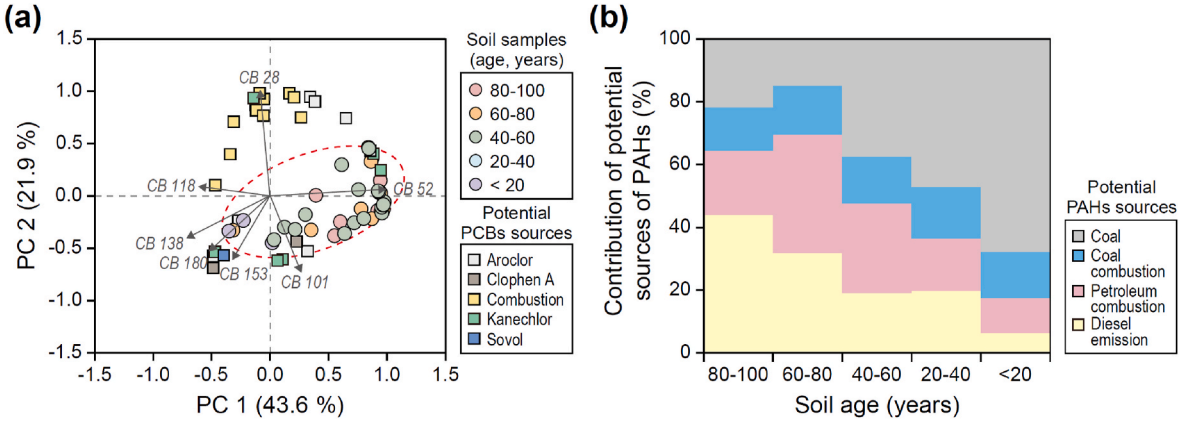

Fig. 3. (a) Source identification of PCBs using principal component analysis (PCA) [source profiles for PCA from Pedersen et al. (2015)]. **(b)** The contribution of potential sources of PAHs, such as diesel emissions, petroleum combustion, coal combustion, and coal, estimated using the PMF model in soils from the glacier foreland of Midtre Lovénbreen, Svalbard. Data from the ML170 site in the soil were excluded due to their influence on result interpretation.

PAHs, with diesel emissions accounting for 44% of the dominant contribution (Fig. 3b and Fig. S5). These sites are located relatively close to Kongsfjorden, where the presence of high-molecular-weight PAHs originating from diesel emissions from various transportation sources is expected. It is important to note that areas near the Kongsfjorden seawater, including these sites, are affected by sea salt originating from that specific region (Kim et al., 2022). In soil samples aged 60–80 years, contamination primarily resulted from petroleum combustion (38%) and diesel emissions (32%). Owing to the persistence of historical pollutants, old soils inherently contain a blend of current and past contaminants. In soil samples aged 40–60 years, PAHs originating from coal (37%) and petroleum combustion (29%) were predominant. Meanwhile, in soils aged 20–40 years, the significant influence of coal combustion in ML170 was deemed to affect the interpretation of the potential sources of PAHs in soils (Fig. S5). Consequently, data from ML170 were excluded. It was observed that the dominant source of PAHs in soils for 20–40 years was coal, constituting 47%. Similarly, coal emerged as the primary PAHs source in soil samples less than 20 years old, accounting for 68%. Based on the analysis of PAHs composition and the PMF model results, it was found that the soil in this area mostly originated from coal and contained mainly coal-related substances. This pattern was more evident in younger soil samples, whereas samples older than 60 years were significantly influenced by human activities. This trend was further evident in the changes in the composition of compounds representing each factor (Factor 1: DbahA; Factor 2: BghiP; Factor 3: BkF; Factor 4: Phe), depending on soil age (Fig. S6). BkF was excluded from the analysis because of the disproportionately large influence of ML170, which could lead to misinterpretation. As the soil age increased, the relative composition of DbahA, BghiP, and BkF increased while the relative composition of Phe decreased. The Phe concentrations in all soil samples remained similar, suggesting a primary base material of coal origin. It can be inferred that it potentially changed due to the accumulation of compounds such as DbahA, BghiP, and BkF in soils over time, influenced by human activities.

When coal is dispersed into the environment, it undergoes a process known as weathering, which involves physical and biochemical changes (Lemkau et al., 2010). The concentration of alkyl-PAHs in the soils was averaged for each soil age (Fig. S7), indicating elevated concentrations of methyl-Na. Methyl-Na can originate from biological sources as well as vegetation fires (Masclet et al., 1987). Although there are no reports of local vegetation fires in this study area, evidence suggests that this region has been influenced by wild forest fires in distant areas (Pakszys and Zielinski, 2017). The distribution pattern of alkyl-PAHs in soils revealed compound-specific outcomes. This is expected because of differences in chemical properties, such as ionization potential, electron affinity, and partition coefficient of individual PAHs in the soils, leading to variations in their degradation and transformation (Gbeddy et al., 2020). Notably, Na, Dbthio, and chrysene (Chr) showed similar bell-shaped distribution patterns, indicative of PAHs originating from coal sources (Hong et al., 2012). In contrast, Flu and Phe exhibited distinct behaviors. Specifically, C2-Flu consistently showed the highest concentration in soils regardless of soil age. Soil samples exposed to atmospheric environments for over 40 years exhibited the highest concentrations of C4-Phe, whereas samples exposed for less than 40 years showed lower C4-Phe concentrations. These findings suggest that Phe underwent significant weathering in soils exposed to the atmosphere for at least 40 years. The origin of alkyl-PAHs was identified using diagnostic double ratios (Fig. 4a). The composition of alkyl-PAHs in soils was found to be similar to that of bituminous coal. These results align with those of a previous study that reported the predominant use of bituminous coal in most areas of Svalbard (Kozak et al., 2013). In addition, the degree of coal weathering in the soils was evaluated (Fig. 4b). Alkyl-PAHs in older soil samples experienced more extensive weathering than those in younger soils. These findings highlight the historical use of bituminous coal in Svalbard and the long-term impact of weathering on these compounds. Significant differences between the sites were observed in the concentrations of PCBs, PAHs, and alkyl-PAHs in the soils of the study area; however, their relative compositions did not show significant differences. Potential sources of pollutants in environmental samples are usually estimated based on their relative compositions (Chan et al., 2011; Wu et al., 2011). Thus, the concentration gradient of pollutants observed in this study is believed to be due to soil characteristics, such as organic matter content and grain size, rather than differences in pollutant sources. Although this study aimed to identify the source of pollutants under the assumption that the composition of soil pollutants is constant, it is important to recognize that pollutants in the soil can be transformed through various physical and biogeochemical processes over time. Future research should consider the dynamic nature of pollutant fate and devise methods to accurately identify pollutant sources.

3.3. Accumulation rate and flux of PTSs in soils

The accumulation rate of PCBs in soils gradually increased as soil age decreased (Fig. 5a). The accumulation flux of PCBs in the soils steadily decreased over time. A previous study observed a decreasing trend in PCB concentrations in environmental samples from Svalbard since the mid-1990s (Aslam et al., 2019) and a gradual decrease in PCB

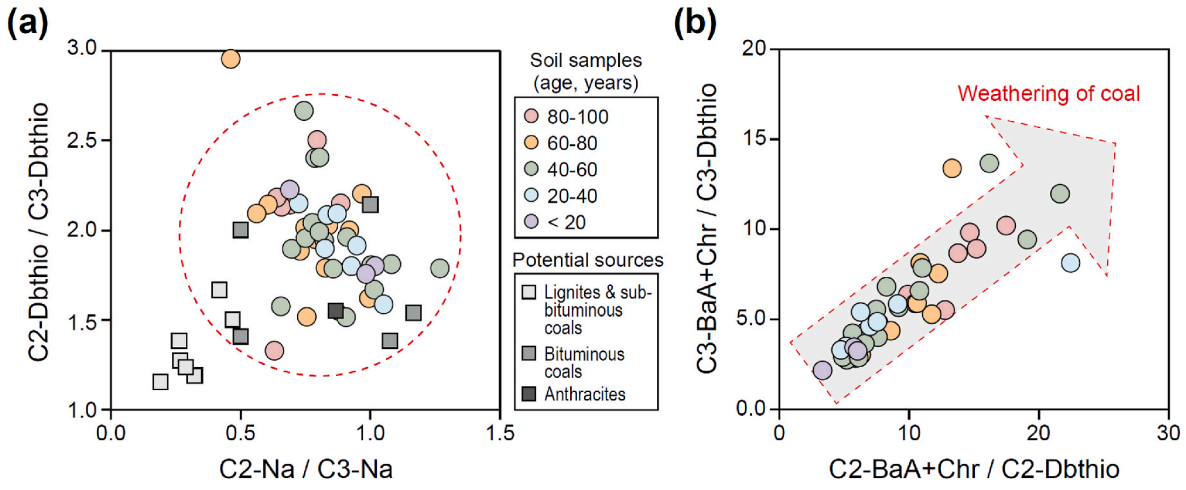

Fig. 4. (a) Diagnostic double ratios (C2–Na/C3–Na and C2-Dbthio/C3-Dbthio) in soil samples from this study and coals reported in previous studies (Hindersmann and Achten, 2018; Pies et al., 2008; Yunker et al., 2002). **(b)** Diagnostic double ratios for weathering characteristics between C2-BaA + Chr/C2-Dbthio and C3-BaA + Chr/C3-Dbthio in soil samples from the glacier foreland of Midtre Lovénbreen, Svalbard.

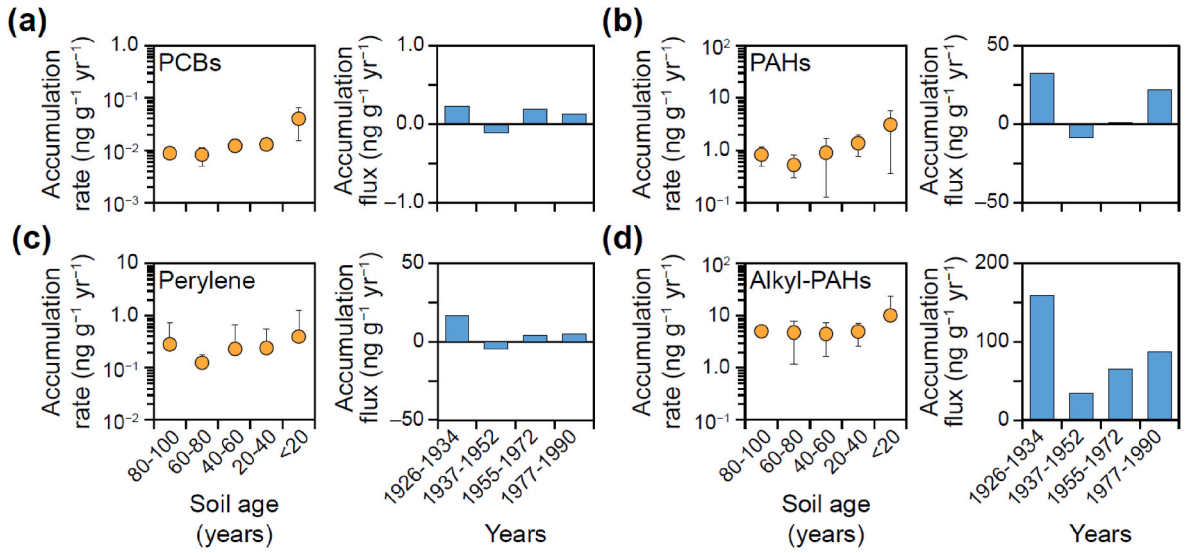

Fig. 5. Accumulation rate and flux of **(a)** PCBs, **(b)** PAHs, **(c)** perylene, and **(d)** alkyl-PAHs in soil samples from the glacier foreland of Midtre Lovénbreen, Svalbard. Data from the ML102 site were excluded.

concentrations in air samples measured at the Zeppelin Observatory in Svalbard between 1998 and 2021 (Fig. S8). Thus, the observed pattern of a high accumulation rate of PCBs in younger soils could be attributed to the deposition of PCBs from air and aerosols onto glaciers, with subglacial materials persisting on the surface soil after glacier retreat (Birks et al., 2017; Zhang et al., 2014a). PCBs are known for their stability and resistance, which means that they can remain stable even after accumulation in glaciers (Mil-Homens et al., 2016). They might have been directly absorbed into the soil rather than being transported into meltwater (Birks et al., 2017). In particular, highly chlorinated CBs may represent such trapping effects, as observed by the relatively high proportion of highly chlorinated CBs in relatively young soils (Fig. S4).

Meanwhile, the concentrations of PAHs, perylene, and alkyl-PAHs in soils were notably higher in ML102 than in the other sites. Considering the potential impact on calculating the accumulation rate and flux in soils of the study area, data from ML102 were excluded. The accumulation rate of PAHs in soils increased as the soil age decreased (Fig. 5b). This is expected to have been influenced not only by PAHs naturally buried in the soils of this area but also by subglacial materials remaining in the soil surface layer after glacier retreat. The accumulation flux of PAHs in the soil was notably high in 1926–1934 and 1977–1990. It is assumed that 1926–1934 was immediately after the start of coal mining operations in Svalbard and was influenced by the active progress of the project (Dowdall et al., 2004). The accumulation flux of PAHs in soils remained constant over time and was high from 1977 to 1990, likely influenced by industrial activity (Garmash et al., 2013; Na et al., 2021).

Predicting changes in the accumulation flux of PAHs in soils in this region is challenging because of recent human activities that have continuously introduced PAHs into the Svalbard region. However, there has been a global reduction in PAH emissions since the mid-1990s (Shen et al., 2013), resulting in decreased PAH concentrations at the Zeppelin Observatory (Fig. S8). These effects are expected to influence the accumulation rate and flux of PAHs in the soil of the study area. The accumulation rate and flux of perylene in the soils were similar to those of PAHs (Fig. 5c). However, for perylene and PAHs in soils, there was a slight difference between the accumulation rate in <20 years and the accumulation flux in 1977–1990. The distribution of perylene in the soil is expected to be more or less regionally and site-specifically distributed rather than increasing or decreasing over time. This suggests the need to investigate naturally occurring perylene, along with the identifiable sources of PAHs in environmental samples from the Arctic region. The accumulation rate of alkyl-PAHs in soils demonstrated a consistent pattern across all soil age groups (Fig. 5d). Additionally, the accumulation flux was consistently high during all the periods. Although the distribution of PTSs may vary based on factors such as region or environmental medium, these results indicate that coal-derived alkyl-PAHs are dominant throughout the Svalbard archipelago. Overall, PAHs and alkyl-PAHs in soils were observed to still exist at high concentrations because of the remains of abandoned coal mines, anthropogenic activities, and naturally buried sources. However, it is still unclear whether the levels of alkyl-PAHs in soils represent background levels in the area or whether they negatively affect organisms in terrestrial ecosystems. While it is acknowledged that determining accumulation rates typically involves calculating compound stocks considering factors such as bulk density and stone content of the soils (Čupr et al., 2010), this study focused solely on computing the concentration change rate of the soils. Despite its limitations, this approach offers valuable insights into the variations in PTS concentrations across different soil age groups.

3.4. Comparison with previous studies

The concentrations of PCBs and PAHs in soils from the Midtre Lovénbreen, Svalbard, were compared with those of other previously reported polar regions (Table 1). The concentration of PCBs in soils in this study was approximately three times lower than that in soils from Ny-Ålesund and London Island in the same region, as reported in a previous study (Zhu et al., 2015). Additionally, the concentrations of PCBs in soils obtained from this study were lower than those in Pyramiden and Bjørnøya but higher than those in Longyearbyen, Svalbard (Ockenden et al., 2003; Jartun et al., 2009). When compared to soils from the Canadian Arctic, the concentration of PCBs in soils in the present study was approximately eight times lower than that of soils from the Distant Early Warning Line, similar to Cornwallis Island, but lower than that of Melville Island, where the concentration was approximately four times higher (Cabrerizo et al., 2018; Stow et al., 2005). The concentrations of PAHs in soils from this study were low compared to previously reported soils from Ny-Ålesund, Billefjorden, and Pyramiden in Svalbard (Gulińska et al., 2003; Marquès et al., 2017; Wang et al., 2009). In addition, in the Russian Arctic, the concentrations of PAHs in soils from this study area were low, except on Vilkitsky Island (Abakumov et al., 2015; Ji et al., 2019). While the number of targeted PCBs and PAHs in this study differed from those in previous studies, the total concentrations of PCBs and PAHs in soils from the Midtre Lovénbreen in Svalbard were observed to be lower than those in soils

Table 1
Concentrations of PCBs and PAHs in soils of Arctic regions obtained from this study and previous studies.

Compounds and country	Region	# of sites	# of targets	Concentrations (ng g^{-1} dw)			References
				Min	Max	Mean	
PCBs							
Norway	Ny-Ålesund (Midtre Lovénbreen)	45	32	0.26	1.1	0.57	This study
	Ny-Ålesund and London Island	7	25	0.57	2.5	1.4	Zhu et al. (2015)
	Pyramiden	31	7	ND[a]	14	1.1	Jartun et al. (2009)
	Longyearbyen	30	7	ND	0.13	0.01	
	Bjørnøya	–	27	4.4	17	–	Ockenden et al. (2003)
Canada	Distant Early Warning Line	21	–	ND	590	4.6	Stow et al. (2005)
	Melville Island	28	70	0.04	0.37	0.12	Cabrerizo et al. (2018)
	Cornwallis Island	8	70	0.06	2.8	0.51	
PAHs							
Norway	Ny-Ålesund (Midtre Lovénbreen)	45	28	14	570	56	This study
	Ny-Ålesund	12	16	37	320	160	Wang et al. (2009)
	Billefjorden	3	15	140	450	250	Gulińska et al. (2003)
	Pyramiden	8	16	53	11,600	2780	Marquès et al. (2017)
Russia	Island Vilkitsky	2	14	–	–	40	Abakumov et al. (2015)
	Islands Izvestii TslK	2	14	–	–	1400	
	Cape Chelyuskin	2	14	–	–	630	
	Island Belyi	2	14	–	–	170	
	Cape Sterligov	2	14	–	–	150	
	Yamal-Nenets autonomous region	41	16	78	130	99	Ji et al. (2019)

[a] ND: Not detected.

from other Arctic regions.

In this study, we conducted a more precise analysis of the distribution patterns of PCBs and PAHs at 45 densely sampled soil sites within the study area. This approach demonstrated that even within the same region, PTS concentrations can vary due to factors such as clay content, SOC content, glacio-fluvial runoff influence, and vegetation. Additionally, this study identified the distribution of emerging PAHs in the soil, which has not been widely analyzed in previous studies (Lee et al., 2023). Emerging PAHs are known to have similar origins, environmental distributions, and potential toxicities as EPA PAHs (Cha et al., 2019; Lee et al., 2023). Future studies should assess the contamination of emerging PAHs that have not been frequently monitored in Arctic soils.

4. Conclusion

This study investigated the chronological distribution and potential sources of PTSs in soils from the glacier foreland of Midtre Lovénbreen, Spitsbergen in Svalbard. The concentration pattern of PTSs in the soil is influenced by global efforts to regulate and reduce PCBs and PAHs. The continued detection of PTSs in relatively young soils may be attributed to their refractory characteristics, ongoing release, and natural origin. More detailed investigations are required to ascertain whether the sources of PTSs in soils are primarily local or are introduced through long-range transport. Among the local sources, it is important to determine whether they are natural or anthropogenic. Furthermore, it is essential to evaluate the potential deformations caused by physical-chemical interactions, such as photooxidation, resulting from the long-range transport of PTSs. The findings of this study provide novel insights into the accumulation patterns, fate, and origin of PTSs, considering soil age and the influence of glacio-fluvial runoff.

CRediT authorship contribution statement

Jihyun Cha: Writing – original draft, Visualization, Investigation, Formal analysis, Data curation, Conceptualization. **Jung-Hyun Kim:** Writing – review & editing, Investigation, Formal analysis, Data curation. **Ji Young Jung:** Writing – review & editing, Investigation, Formal analysis. **Seung-Il Nam:** Writing – review & editing, Project administration, Funding acquisition. **Seongjin Hong:** Writing – review & editing, Visualization, Supervision, Project administration, Investigation, Funding acquisition, Formal analysis, Conceptualization.

Declaration of competing interest

The authors declare that they have no known competing financial interests or personal relationships that could have appeared to influence the work reported in this paper.

Data availability

Data will be made available on request.

Acknowledgments

This research was supported by the National Research Foundation of Korea (NRF) Grant funded by the Korean Government (MIST; the Ministry of Science and ICT; NRF-2021M1A5A1075514) (KOPRI-PN24013).

Appendix A. Supplementary data

Supplementary data to this article can be found online at https://doi.org/10.1016/j.envpol.2024.124387.

References

Aichner, B., Bussian, B.M., Lehnik-Habrink, R., Hein, S., 2015. Regionalized concentrations and fingerprints of polycyclic aromatic hydrocarbons (PAHs) in German forest soils. Environ. Pollut. 203, 31–39. https://doi.org/10.1016/j.envpol.2015.03.026.

Abakumov, E.V., Tomashunas, V.M., Lodygin, E.D., Gabov, D.N., Sokolov, V.T., Krylenkov, V.A., Kirtsideli, I.Y., 2015. Polycyclic aromatic hydrocarbons in insular and coastal soils of the Russian Arctic. Eurasian Soil Sci. 48, 1300–1305. https://doi.org/10.1134/S1064229315120029.

Ai, S., Ding, X., Tolle, F., Wang, Z., Zhao, X., 2019. Latest Geodetic changes of Austre Lovénbreen and Pedersenbreen, Svalbard. Rem. Sens. 11, 2890. https://doi:10.3390/rs11242890.

Aslam, S.N., Huber, C., Asimakopoulos, A.G., Steinnes, E., Mikkelsen, Ø., 2019. Trace elements and polychlorinated biphenyls (PCBs) in terrestrial compartments of Svalbard, Norwegian Arctic. Sci. Total Environ. 685, 1127–1138. https://doi.org/10.1016/j.scitotenv.2019.06.060.

Bakhtiari, A.R., Zakaria, M.P., Ramin, M., Yaziz, M.I., Lajis, M.N.H., Bi, X., 2010. Characterization of perylene in Tropical environment: comparison of New and old fungus comb for identifying perylene precursor in *Macrotermes gilvus* termite nests of peninsular Malaysia. Environment (Wash. D C) 3, 13–19.

Birks, S.J., Cho, S., Taylor, E., Yi, Y., Gibson, J.J., 2017. Characterizing the PAHs in surface waters and snow in the Athabasca region: implications for identifying hydrological pathways of atmospheric deposition. Sci. Total Environ. 603–604, 570–583. https://doi.org/10.1016/j.scitotenv.2017.06.051.

Cabrerizo, A., Muir, D.C.G., De Silva, A.O., Wang, X., Lamoureux, S.F., Lafrenière, M.J., 2018. Legacy and emerging persistent organic pollutants (POPs) in terrestrial

compartments in the high arctic: sorption and secondary sources. Environ. Sci. Technol. 52, 14187–14197. https://doi.org/10.1021/acs.est.8b05011.
Casal, P., Cabrerizo, A., Vila-Costa, M., Pizarro, M., Jiménez, B., Dachs, J., 2018. Pivotal role of snow deposition and melting driving fluxes of polycyclic aromatic hydrocarbons at coastal livingston island (Antarctica). Environ. Sci. Technol. 52, 12327–12337. https://doi.org/10.1021/acs.est.8b03640.
Cha, J., Hong, S., Kim, J., Lee, J., Yoon, S.J., Lee, S., Moon, H.B., Shin, K.H., Hur, J., Giesy, J.P., Khim, J.S., 2019. Major AhR-active chemicals in sediments of Lake Sihwa, South Korea: application of effect-directed combined with full-scan screening analysis. Environ. Int. 133, 105199 https://doi.org/10.1016/j.envint.2019.105199.
Chan, Y.c., Hawas, O., Hawker, D., Vowles, P., Cohen, D.D., Stelcer, E., Simpson, R., Golding, G., Christensen, E., 2011. Using multiple type composition data and wind data in PMF analysis to apportion and locate sources of air pollutants. Atmos. Environ. 45, 439–449. https://doi:10.1016/j.atmosenv.2010.09.060.
Čupr, P., Bartoš, T., Sáňka, M., Klánová, J., Mikeš, O., Holoubek, I., 2010. Soil burdens of persistent organic pollutants – their levels, fate and risks Part III. Quantification of the soil burdens and related health risks in the Czech Republic. Sci. Total Environ. 408, 486–494. https://doi.org/10.1016/j.scitotenv.2009.09.049.
Dowdall, M., Vicat, K., Frearson, I., Gerland, S., Lind, B., Shaw, G., 2004. Assessment of the radiological impacts of historical coal mining operations on the environment of Ny-Ålesund, Svalbard. J. Environ. Radioact. 71, 101–114. https://doi.org/10.1016/S0265-931X(03)00144-9.
Eckhardt, S., Breivik, K., Manø, S., Stohl, A., 2007. Record high peaks in PCB concentrations in the Arctic atmosphere due to long-range transport of biomass burning emissions. Atmos. Chem. Phys. 7, 4527–4536. https://doi.org/10.5194/acp-7-4527-2007.
Eichel, J., Corenblit, D., Dikau, R., 2015. Conditions for feedbacks between geomorphic and vegetation dynamics on lateral moraine slopes: a biogeomorphic feedback window. Earth Surf. Process. Landforms 41, 406–419. https://doi.org/10.1002/esp.3859.
Fang, S., Cui, Q., Matherne, B., Hou, A., 2017. Polychlorinated biphenyl concentrations, accumulation rates in soil from atmospheric deposition and analysis of their affecting landscape variables along an urban-rural gradient in Shanghai, China. Chemosphere 186, 884–892. https://doi.org/10.1016/j.chemosphere.2017.08.059.
Garmash, O., Hermanson, M.H., Isaksson, E., Schwikowski, M., Divine, D., Teixeira, C., Muir, D.C.G., 2013. Deposition history of polychlorinated biphenyls to the lomonosovfonna glacier, svalbard: a 209 congener analysis. Environ. Sci. Technol. 47, 12064–12072. https://doi.org/10.1021/es402430t.
Gbeddy, G., Goonetilleke, A., Ayoko, G.A., Egodawatta, P., 2020. Transformation and degradation of polycyclic aromatic hydrocarbons (PAHs) in urban road surfaces: influential factors, implications and recommendations. Environ. Pollut. 257, 113510 https://doi.org/10.1016/j.envpol.2019.113510.
Gocht, T., Barth, J.A.C., Epp, M., Jochmann, M., Blessing, M., Schmidt, T.C., Grathwohl, P., 2007. Indications for pedogenic formation of perylene in a terrestrial soil profile: depth distribution and first results from stable carbon isotope ratios. Appl. Geochem. 22, 2652–2263. https://doi:10.1016/j.apgeochem.2007.06.004.
Gulińska, J., Rachlewicz, G., Szczucinski, W., Baralkiewicz, D., Kózka, M., Bulska, E., Burzyk, M., 2003. Soil contamination in high Arctic areas of human impact, central Spitsbergen, Svalbard. Pol. J. Environ. Stud. 12, 701–707.
Harrison, R.M., Smith, D.J.T., Luhana, L., 1996. Source apportionment of atmospheric polycyclic aromatic hydrocarbons collected from an urban location in birmingham, U.K. Environ. Sci. Technol. 30, 825–832. https://doi.org/10.1021/es950252d.
Hermanson, M.H., Isaksson, E., Divine, D., Teixeira, C., Muir, D.C.G., 2020. Atmospheric deposition of polychlorinated biphenyls to seasonal surface snow at four glacier sites on Svalbard, 2013–2014. Chemosphere 243, 125324. https://doi.org/10.1016/j.chemosphere.2019.125324.
Hindersmann, B., Achten, C., 2018. Urban soils impacted by tailings from coal mining: PAH source identification by 59 PAHs, PBCA and alkylated PAHs. Environ. Pollut. 242, 1217–1225. doi.org/10.1016/j.envpol.2018.08.014.
Hong, S., Khim, J.S., Ryu, J., Park, J., Song, S.J., Kwon, B.-O., Choi, K., Ji, K., Seo, J., Lee, S., Park, J., Lee, W., Choi, Y., Lee, K.T., Kim, C.-K., Shim, W.J., Naile, J.E., Giesy, J.P., 2012. Two years after the hebei spirit oil spill: residual crude-derived hydrocarbons and potential AhR-mediated activities in coastal sediments. Environ. Sci. Technol. 46, 1406–1414. https://doi.org/10.1021/es203491b.
Howaniec, N., Kuna-Gwoździewicz, P., Smoliński, A., 2018. Assessment of emission of selected gaseous components from coal processing waste storage site. Sustainability 10. https://doi.org/10.3390/su10030744.
Jartun, M., Ottesen, R.T., Volden, T., Lundkvist, Q., 2009. Local sources of polychlorinated biphenyls (PCB) in Russian and Norwegian settlements on spitsbergen island, Norway. J. Toxicol. Environ. Health A 72, 284–294. https://doi.org/10.1080/15287390802539426.
Ji, X., Abakumov, E., Polyako, V., Xie, X., Dongyang, W., 2019. The ecological impact of mineral exploitation in the Russian Arctic: a field-scale study of polycyclic aromatic hydrocarbons (PAHs) in permafrost-affected soils and lichens of the Yamal-Nenets autonomous region. Environ. Pollut. 255, 113239 https://doi.org/10.1016/j.envpol.2019.113239.
Jiao, L., Zheng, G.J., Minh, T.B., Richardson, B., Chen, L., Zhang, Y., Yeung, L.W., Lam, J. C.W., Yang, X., Lam, P.K.S., Wong, M.H., 2009. Persistent toxic substances in remote lake and coastal sediments from Svalbard, Norwegian Arctic: levels, sources and fluxes. Environ. Pollut. 157, 1342–1351. https://doi:10.1016/j.envpol.2008.11.030.
Khedim, N., Cécillon, L., Paulenard, J., Barré, P., Baudin, F., Marta, S., Rabatel, A., Dentant, C., Cauvy-Fraunié, S., Anthelme, F., Gielly, L., Ambrosini, R., Franzetti, A., Azzoni, R.S., Caccianiga, M.S., Compostella, C., Clague, J., Tielidze, L., Messager, E., Choler, P., Ficetola, G.F., 2021. Topsoil organic matter build-up in glacier forelands around the world. Global Change Biol. 27, 1662–1677. https://doi.org/10.1111/gcb.15496.
Kim, Y., Hong, S., Lee, J., Yoon, S.J., An, Y., Kim, M.-S., Jeong, H.-D., Khim, J.S., 2021. Spatial distribution and source identification of traditional and emerging persistent toxic substances in the offshore sediment of South Korea. Sci. Total Environ. 789, 147996 https://doi.org/10.1016/j.scitotenv.2021.147996.
Kim, Y.J., Laffly, D., Kim, S.-e., Nilsen, L., Chi, J., Nam, S., Lee, Y.B., Jeong, S., Mishra, U., Lee, Y.K., Jung, J.Y., 2022. Chronological changes in soil biogeochemical properties of the glacier foreland of Midtre Lovénbreen, Svalbard, attributed to soil-forming factors. Geoderma 415, 115777. https://doi.org/10.1016/j.geoderma.2022.115777.
Kozak, K., Polkowska, Ż., Ruman, M., Kozioł, K., Namieśnik, J., 2013. Analytical studies on the environmental state of the Svalbard Archipelago provide a critical source of information about anthropogenic global impact. Trac-Trend. Anal. Chem. 50, 107–126. https://doi.org/10.1016/j.trac.2013.04.016.
Lee, J., Cha, J., Yoon, S.J., Hong, S., Khim, J.S., 2022. Instrumental and bioanalytical characterization of dioxin-like activity in sediments from the Yeongsan River and the Nakdong River estuaries, South Korea. Sci. Total Environ. 826, 154240 https://doi.org/10.1016/j.scitotenv.2022.154240.
Lee, J., Kim, Y., Cha, J., Kim, D., Jang, K., Kim, J.-H., Nam, S.-I., Hong, S., 2023. Distributions and potential sources of polychlorinated biphenyls and polycyclic aromatic hydrocarbons in the glacimarine sediments of Arctic Svalbard. Mar. Pollut. Bull. 189, 114740 https://doi.org/10.1016/j.marpolbul.2023.114740.
Lemkau, K.L., Peacock, E.E., Nelson, R.K., Ventura, G.T., Kovecses, J.L., Reddy, C.M., 2010. The M/V *Cosco Busan* spill: source identification and short-term fate. Mar. Pollut. Bull. 60, 2123–2129. https://doi.org/10.1016/j.marpolbul.2010.09.001.
Li, Q., Xiao, P., Shen, D., Huang, Y., Shi, X., Li, X., Liu, Y., 2023. Level and risk assessment of selected polychlorinated biphenyls, polycyclic aromatic hydrocarbons, and organochlorine pesticides in walnut and soil. Environ. Sci. Pollut. Res. 30, 14849–14859. https://doi.org/10.1007/s11356-022-23158-7.
Li, Y., Wang, G., Wang, J., Jia, Z., Zhou, Y., Wang, C., Li, Y., Zhou, S., 2019. Determination of influencing factors on historical concentration variations of PAHs in West Taihu Lake, China. Environ. Pollut. 249, 573–580. https://doi.org/10.1016/j.envpol.2019.03.055.
Liu, C., Gu, C., Yu, K., Li, H., Teppen, B.J., Johnston, C.T., Boyd, S.A., Zhou, D., 2015. Integrating structural and thermodynamic mechanisms for sorption of PCBs by montmorillonite. Environ. Sci. Technol. 49, 2796–2805. https://doi.org/10.1021/es505205p.
Lynas, M., Houlton, B.Z., Perry, S., 2021. Greater than 99% consensus on human caused climate change in the peer-reviewed scientific literature. Environ. Res. Lett. 16, 114005 https://doi.org/10.1088/1748-9326/ac2966.
Ma, J., Hung, H., Macdonald, R.W., 2016. The influence of global climate change on the environmental fate of persistent organic pollutants: a review with emphasis on the Northern Hemisphere and the Arctic as a receptor. Global Planet. Change 146, 89–108. https://doi.org/10.1016/j.gloplacha.2016.09.011.
Marquès, M., Sierra, J., Drotikova, T., Mari, M., Nadal, M., Domingo, J.L., 2017. Concentrations of polycyclic aromatic hydrocarbons and trace elements in Arctic soils: a case-study in Svalbard. Environ. Res. 159, 202–211. https://doi.org/10.1016/j.envres.2017.08.003.
Masclet, P., Bresson, M.A., Mouvier, G., 1987. Polycyclic aromatic hydrocarbons emitted by power stations, and influence of combustion sources. Fuel 66, 556–562. https://doi.org/10.1016/0016-2361(87)90163-3.
Mil-Homens, M., Vicente, M., Grimalt, J.O., Micaelo, C., Abrantes, F., 2016. Reconstruction of organochlorine compound inputs in the Tagus Prodelta. Sci. Total Environ. 540, 231–240. https://doi.org/10.1016/j.scitotenv.2015.07.009.
Miner, K.R., D'Andrilli, J., Mackelprang, R., Edwards, A., Malaska, M.J., Waldrop, M.P., Miller, C.E., 2021. Emergent biogeochemical risks from Arctic permafrost degradation. Nat. Clim. Change 11, 809–819. https://doi.org/10.1038/s41558-021-01162-y.
Moon, K.J., Han, J.S., Ghim, Y.S., Kim, Y.J., 2008. Source apportionment of fine carbonaceous particles by positive matrix factorization at Gosan background site in East Asia. Environ. Int. 34, 654–664. https://doi.org/10.1016/j.envint.2007.12.021.
Moreau, M., Laffly, D., Joly, D., Brossard, T., 2005. Analysis of plant colonization on an arctic moraine since the end of the Little Ice Age using remotely sensed data and a Bayesian approach. Remote Sens. Environ. 99, 244–253. https://doi:10.1016/j.rse.2005.03.017.
Na, G., Liang, Y., Li, R., Gao, H., Jin, S., 2021. Flux of polynuclear aromatic compounds (PAHs) from the atmosphere and from reindeer/bird feces to arctic soils in ny-Ålesund (Svalbard). Arch. Environ. Contam. Toxicol. 81, 166–181. https://doi.org/10.1007/s00244-021-00851-1.
Nuth, C., Kohler, J., König, M., von Deschwanden, A., Hagen, J.O., Kääb, A., Moholdt, G., Pettersson, R., 2013. Decadal changes from a multi-temporal glacier inventory of Svalbard. Cryosphere 7, 1603–1621. https://doi:10.5194/tc-7-1603-2013.
Ockenden, W.A., Breivik, K., Meijer, S.N., Steinnes, E., Sweetman, A.J., Jones, K.C., 2003. The global re-cycling of persistent organic pollutants is strongly retarded by soils. Environ. Pollut. 121, 75–80. https://doi.org/10.1016/S0269-7491(02)00204-X.
Opuene, K., Agbozu, I.E., Ekeh, L.E., 2007. Identification of perylene in sediments: occurrence and diagenetic evolution. Int. J. Environ. Sci. Te. 4, 457–462. https://doi.org/10.1007/BF03325981.
Pakszys, P., Zielinski, T., 2017. Aerosol optical properties over svalbard: a comparison between ny-Ålesund and hornsund. Oceanologia 59, 431–444. https://doi.org/10.1016/j.oceano.2017.05.002.
Pedersen, K.B., Lejon, T., Jensen, P.E., Ottosen, L.M., 2015. Chemometric analysis for pollution source assessment of harbour sediments in arctic locations. Water Air Soil Pollut. 226, 150. https://doi.org/10.1007/s11270-015-2416-4.
Pies, C., Hoffmann, B., Petrowsky, J., Yang, Y., Ternes, T.A., Hofmann, T., 2008. Characterization and source identification of polycyclic aromatic hydrocarbons

(PAHs) in river bank soils. Chemosphere 72, 1594–1601. https://doi.org/10.1016/j.chemosphere.2008.04.021.
Qu, Y., Gong, Y., Ma, J., Wei, H., Liu, Q., Liu, L., Wu, H., Yang, S., Chen, Y., 2020. Potential sources, influencing factors, and health risks of polycyclic aromatic hydrocarbons (PAHs) in the surface soil of urban park in Beijing, China. Environ. Pollut. 260, 114016.
Rantanen, M., Karpechko, A.Y., Lipponen, A., Nordling, K., Hyvärinen, O., Ruosteenoja, K., Vihma, T., Laaksonen, A., 2022. The Arctic has warmed nearly four times faster than the globe since 1979. Commun. Earth Environ. 3, 168. https://doi.org/10.1038/s43247-022-00498-3.
Ravindra, K., Sokhi, R., Van Grieken, R., 2008. Atmospheric polycyclic aromatic hydrocarbons: source attribution, emission factors and regulation. Atmos. Environ. 42, 2895–2921. https://doi.org/10.1016/j.atmosenv.2007.12.010.
Schellnhuber, H.J., Rahmstorf, S., Winkelmann, R., 2016. Why the right climate target was agreed in Paris. Nat. Clim. Change 6, 649–653. https://doi.org/10.1038/nclimate3013.
Shen, H., Huang, Y., Wang, R., Zhu, D., Li, W., Shen, G., Wang, B., Zhang, Y., Chen, Y., Lu, Y., Chen, H., Li, T., Sun, K., Li, B., Liu, W., Liu, J., Tao, S., 2013. Global atmospheric emissions of polycyclic aromatic hydrocarbons from 1960 to 2008 and future predictions. Environ. Sci. Technol. 47, 6415–6424. https://doi.org/10.1021/es400857z.
Sims, R.C., Overcash, M.R., 1983. Fate of polynuclear aromatic compounds (PNAs) in soil-plant systems. Res. Rev. 88, 1–68. https://doi.org/10.1007/978-1-4612-5569-7_1.
Steenhuisen, F., van den Heuvel-Greve, M., 2021. Exposure radius of a local coal mine in an Arctic coastal systems; correlation between PAHs and mercury as a marker for a local mercury source. Environ. Monit. Assess. 193, 499. https://doi.org/10.1007/s10661-021-09287-5.
Stow, J.P., Sova, J., Reimer, K.J., 2005. The relative influence of distant and local (DEW-line) PCB sources in the Canadian Arctic. Sci. Total Environ. 342, 107–118. https://doi:10.1016/j.scitotenv.2004.12.028.
Ubl, S., Scheringer, M., Hungerbühler, K., 2017. Relationships between atmospheric transport regimes and PCB concentrations in the air at Zeppelin, spitsbergen. Environ. Sci. Technol. 51, 9784–9791. https://doi.org/10.1021/acs.est.7b02571.
Venkatachalam, S., Kannan, V.M., Saritha, V.N., Loganathachetti, D.S., Mohan, M., Krishnan, K.P., 2021. Bacterial diversity and community structure along the glacier foreland of Midtre Lovénbreen, Svalbard, Arctic. Ecol. Indicat. 126, 107704 https://doi.org/10.1016/j.ecolind.2021.107704.
Wang, Z., Ma, X., Na, G., Lin, Z., Ding, Q., Yao, Z., 2009. Correlations between physicochemical properties of PAHs and their distribution in soil, moss and reindeer dung at Ny-Ålesund of the Arctic. Environ. Pollut. 3132–3136. https://doi:10.1016/j.envpol.2009.05.014.
Wania, F., Haugen, J.-E., Lei, Y.D., Mackay, D., 1998. Temperature dependence of atmospheric concentrations of semivolatile organic compounds. Environ. Sci. Technol. 32, 1013–1021. https://doi.org/10.1021/es970856c.
Wania, F., Mackay, D., 1996. Tracking the distribution of persistent organic pollutants. Environ. Sci. Technol. 30, 390–396.
Wania, F., Westgate, J.N., 2008. On the mechanism of mountain cold-trapping of organic chemicals. Environ. Sci. Technol. 42, 9092–9098. https://doi.org/10.1021/es8013198.
Wilcke, W., 2007. Global patterns of polycyclic aromatic hydrocarbons (PAHs) in soil. Geoderma 141, 157–166. https://doi.org/10.1016/j.geoderma.2007.07.007.
Wild, B., Schnecker, J., Alves, R.J.E., Barsukov, P., Bárta, J., Čapek, P., Gentsch, N., Gittel, A., Guggenberger, G., Lashchinskiy, N., Mikutta, R., Rusalimova, O., Šantrůčková, H., Shibistova, O., Urich, T., Watzka, M., Zrazhevskaya, G., Richter, A., 2014. Input of easily available organic C and N stimulates microbial decomposition of soil organic matter in arctic permafrost soil. Soil Biol. Biochem. 75, 143–151. https://doi.org/10.1016/j.soilbio.2014.04.014.
Wu, S., Xia, X., Yang, L., Liu, H., 2011. Distribution, source and risk assessment of polychlorinated biphenyls (PCBs) in urban soils of Beijing, China. Chemosphere 82, 732–738. https://doi:10.1016/j.chemosphere.2010.10.090.
Yang, Y., Tao, S., Zhang, N., Zhang, D.Y., Li, X.Q., 2010. The effect of soil organic matter on fate of polycyclic aromatic hydrocarbons in soil: a microcosm study. Environ. Pollut. 158, 1768–1774. https://doi:10.1016/j.envpol.2009.11.010.
Yu, Y., Katsoyiannis, A., Bohlin-Nizzetto, P., Brorström-Lundén, E., Ma, J., Zhao, Y., Wu, Z., Tych, W., Mindham, D., Sverko, E., Barresi, E., Dryfhout-Clark, H., Fellin, P., Hung, H., 2019. Polycyclic aromatic hydrocarbons not declining in arctic air despite global emission reduction. Environ. Sci. Technol. 53, 2375–2382. https://doi.org/10.1021/acs.est.8b05353.
Yunker, M.B., Macdonald, R.W., Vingarzan, R., Mitchell, R.H., Goyette, D., Sylvestre, S., 2002. PAHs in the Fraser River basin: a critical appraisal of PAH ratios as indicators of PAH source and composition. Org. Geochem. 33, 489–515. https://doi.org/10.1016/S0146-6380(02)00002-5.
Zhang, P., Ge, L., Gao, H., Yao, T., Fang, X., Zhou, C., Na, G., 2014a. Distribution and transfer pattern of Polychlorinated Biphenyls (PCBs) among the selected environmental media of Ny-Ålesund, the Arctic: as a case study. Mar. Pollut. Bull. 89, 267–275. https://doi.org/10.1016/j.marpolbul.2014.09.050.
Zhang, X., Xu, Y., Ruan, J., Ding, S., Huang, X., 2014b. Origin, distribution and environmental significance of perylene in Okinawa Trough since last glaciation maximum. Org. Geochem. 76, 288–294. https://doi.org/10.1016/j.orggeochem.2014.09.008.
Zhu, C., Li, Y., Wang, P., Chen, Z., Ren, D., Ssebugere, P., Zhang, Q., Jiang, G., 2015. Polychlorinated biphenyls (PCBs) and polybrominated biphenyl ethers (PBDEs) in environmental samples from Ny-Ålesund and London Island, Svalbard, the Arctic. Chemosphere 126, 40–46. https://doi.org/10.1016/j.chemosphere.2015.01.043.

<Environmental Pollution>

Supplementary materials for

Chronological distribution and potential sources of persistent toxic substances in soils from the glacier foreland of Midtre Lovénbreen, Svalbard

Jihyun Cha, Jung-Hyun Kim, Ji Young Jung, Seung-Il Nam, Seongjin Hong*

This file includes:

Number of pages: 25

Supplementary Text

Number of Supplementary Tables: 6; Tables S1 to S6

Number of Supplementary Figures: 8; Figs. S1 to S8

References

***Corresponding author.** *E-mail*: hongseongjin@cnu.ac.kr (S. Hong).

Supplementary Text

Soil Organic Carbon, Total Nitrogen, and Grain Size Distributions. The soil organic carbon (SOC) content from the Midtre Lovénbreen glacier foreland ranged from 0.07% to 0.96%, with a mean of 0.37% (Fig. S1 and Table S1) (Kim et al., 2022). SOC contents were notably observed to increase with soil age, attributed to processes such as glacier retreat, soil exposure, vegetation establishment, and more organic matter accumulation. Specifically, it is expected that the SOC content, relative to soil age, would be predominantly influenced by the frequency of vegetation presence, including lichens, bryophytes, *Saxifraga oppositifolia*, and *Salix Polaris* (Kim et al., 2022). The SOC content was approximately 1.7 times higher in no-runoff sites than in runoff sites. Noteworthy among the no-runoff sites were ML120 (0.96%), ML71 (0.87%), and ML102 (0.83%), which exhibited high SOC content. The SOC content in Arctic regions is mainly influenced by increased vegetation cover in the surface layer (Wietrzyk et al., 2018). Similarly, the total nitrogen (TN) content in the soil showed an increasing trend across the chronological sequence of soil samples. TN content is generally affected by cyanobacteria and organic debris from plants in soil samples (Pessi et al., 2019). The C/N ratio in the soils ranged from 9.3 to 23, with a mean of 14 (Fig. S1) (Kim et al., 2022). Soil organic matter (SOM) in the soils in this study area was mainly identified as being in a state of mineralization or equilibrium. The mineralization of SOM in the soil is significantly influenced by regional temperature, with slower processes occurring at temperatures below 10 ℃ (Brust, 2019; Leirós et al., 1999). Given that the annual temperature in Svalbard is –12 to 5.2 ℃, SOM mineralization in the soil from this study area is expected to be relatively slow (Førland et al., 2011). The average grain size composition of the soils was 70% sand, 25% silt, and 5.0% clay (Fig. S1) (Kim et al., 2022). Soil samples from the runoff sites showed higher sand content, likely due to the washout of lighter silt and clay. These variations in grain size could affect SOC through the differential transport and distribution of particles. Thus, the influence of glacio-fluvial runoff in this study area is expected to be a key factor in altering and shaping soil properties.

Supplementary Tables

Table S1. Overview of sampling locations and properties of soil samples from the glacier foreland of Midtre Lovénbreen, Svalbard. Data for soil organic carbon, total nitrogen, and grain size were reported in a previous study (Kim et al., 2022).

Samples	Sampling date	Latitude (°N)	Longitude (°E)	Soil age (year)	Retreat year	SOC[a] (%)	TN[b] (%)	Sand (%)	Silt (%)	Clay (%)	Runoff/ No-runoff
ML 6	2014.07.22	78.9057	12.0766	88	1926	0.19	0.01	88	10	2.3	No-runoff
ML 204	2014.07.09	78.8993	12.1083	88	1926	0.33	0.02	89	8.8	2.6	Runoff
ML 263	2014.07.09	78.8960	12.1054	85	1929	0.71	0.04	68	29	3.1	No-runoff
ML 66	2014.07.17	78.9028	12.0264	84	1930	0.68	0.04	84	15	1.6	No-runoff
ML 10	2014.07.17	78.9051	12.0437	83	1931	0.39	0.02	61	32	6.8	No-runoff
ML 177	2014.07.09	78.9002	12.1007	81	1933	0.25	0.02	53	38	9.6	No-runoff
ML 71	2014.07.14	78.9033	12.0873	80	1934	0.87	0.06	58	32	10	No-runoff
ML 20	2014.07.22	78.9050	12.0792	77	1937	0.49	0.04	86	12	1.7	No-runoff
ML 25	2014.07.22	78.9047	12.0708	73	1941	0.31	0.02	78	13	8.5	No-runoff
ML 37	2014.07.17	78.9039	12.0371	72	1942	0.39	0.04	66	28	6.2	No-runoff
ML 298	2014.07.09	78.8915	12.0952	71	1943	0.44	0.03	60	32	8.5	No-runoff
ML 47	2014.07.22	78.9040	12.0781	70	1944	0.67	0.06	70	27	2.7	No-runoff
ML 130	2014.07.13	78.9015	12.0896	66	1948	0.40	0.03	85	11	3.4	Runoff
ML 62	2014.07.22	78.9034	12.0734	65	1949	0.52	0.03	85	14	1.8	Runoff
ML 279	2014.07.09	78.8942	12.0940	65	1949	0.16	0.01	90	8.0	1.6	Runoff
ML 60	2014.07.16	78.9034	12.0619	64	1950	0.75	0.05	54	36	10	No-runoff
ML 102	2014.07.17	78.9017	12.0294	64	1950	0.83	0.03	42	42	17	No-runoff
ML 149	2014.07.13	78.9009	12.0875	63	1951	0.07	0.01	98	1.6	0.80	Runoff
ML 81	2014.07.17	78.9025	12.0369	62	1952	0.26	0.02	93	5.3	1.7	No-runoff
ML 84	2014.07.16	78.9027	12.0660	59	1955	0.20	0.01	90	7.9	2.4	No-runoff
ML 141	2014.07.14	78.9011	12.0821	58	1956	0.07	0.005	97	1.3	1.8	Runoff
ML 103	2014.07.14	78.9021	12.0712	57	1957	0.59	0.03	62	31	6.9	No-runoff
ML 222	2014.07.12	78.8984	12.0910	57	1957	0.64	0.04	55	34	11	No-runoff
ML 93	2014.07.16	78.9022	12.0457	54	1960	0.07	0.01	90	7.7	1.8	Runoff
ML 120	2014.07.14	78.9016	12.0728	54	1960	0.96	0.04	66	27	7.5	No-runoff
ML 132	2014.07.14	78.9013	12.0739	53	1961	0.56	0.03	50	38	12	No-runoff
ML 231	2014.07.12	78.8979	12.0887	51	1963	0.31	0.02	78	19	3.4	No-runoff
ML 253	2014.07.12	78.8966	12.0920	49	1965	0.20	0.01	86	13	0.96	No-runoff
ML 124	2014.07.16	78.9013	12.0476	48	1966	0.44	0.02	57	34	9.0	No-runoff
ML 266	2014.07.12	78.8956	12.0910	48	1966	0.44	0.02	88	10	1.8	Runoff
ML 138	2014.07.16	78.9009	12.0593	45	1969	0.31	0.02	46	47	7.5	Runoff
ML 252	2014.07.12	78.8967	12.0888	45	1969	0.17	0.01	93	6.0	1.2	Runoff
ML 157	2014.07.15	78.9004	12.0650	44	1970	0.24	0.02	79	19	2.0	Runoff

ML 182	2014.07.15	78.8997	12.0715	44	1970	0.29	0.01	60	33	6.5	No-runoff
ML 292	2014.07.10	78.8925	12.0899	42	1972	0.28	0.02	53	40	7.1	No-runoff
ML 225	2014.07.13	78.8981	12.0772	37	1977	0.13	0.01	60	33	6.5	No-runoff
ML 274	2014.07.10	78.8947	12.0856	37	1977	0.34	0.02	54	37	9.0	No-runoff
ML 191	2014.07.15	78.8993	12.0646	36	1978	0.41	0.03	60	35	5.0	No-runoff
ML 170	2014.07.16	78.8998	12.0445	35	1979	0.15	0.01	89	9.7	1.6	No-runoff
ML 237	2014.07.13	78.8975	12.0769	33	1981	0.22	0.02	59	33	7.9	Runoff
ML 287	2014.07.10	78.8931	12.0832	25	1989	0.30	0.02	35	60	4.6	No-runoff
ML 245	2014.07.13	78.8970	12.0730	24	1990	0.18	0.01	68	29	2.7	Runoff
ML 302	2014.07.15	78.8975	12.0523	11	2003	0.14	0.01	52	36	12	No-runoff
ML 301	2014.07.15	78.8967	12.0632	8	2006	0.24	0.01	50	47	2.6	No-runoff
ML 303	2014.07.15	78.8964	12.0476	3	2011	0.11	0.01	50	39	11	No-runoff

[a] SOC: Soil organic carbon.
[b] TN: Total nitrogen.

Table S2. Target compounds, abbreviations, and target ions in instrumental analysis and method detection limits and recoveries of surrogate standards.

Target compounds	Abbreviation	Quantification ion	Confirmation ion	Method detection limit (ng g^{-1} dw)
Polychlorinated biphenyls (PCBs)				
2,4'-Dichlorobiphenyl	CB 8	222	224	0.01
2,4,4'-Trichlorobiphenyl	CB 28	256	258	0.03
2,2',5,5'-Tetrachlorobiphenyl	CB 52	292	290	0.02
2,2',4,5'-Tetrachlorobiphenyl	CB 49	292	290	0.02
2,2',3,5'-Tetrachlorobiphenyl	CB 44	292	290	0.03
3,4,4'-Trichlorobiphenyl	CB 37	256	258	0.02
2,4,4',5-Tetrachlorobiphenyl	CB 74	292	290	0.02
2,3',4',5-Tetrachlorobiphenyl	CB 70	292	290	0.01
2,3',4,4'-Tetrachlorobiphenyl	CB 66	292	290	0.03
2,3,4,4'-Tetrachlorobiphenyl	CB 60	292	290	0.03
2,2',4,5,5'-Pentachlorobiphenyl	CB 101	326	324	0.02
2,2',4,4',5-Pentachlorobiphenyl	CB 99	326	328	0.02
2,2',3,4,5'-Pentachlorobiphenyl	CB 87	292	290	0.02
3,3',4,4'-Tetrachlorobiphenyl	CB 77	326	256	0.01
2,2',3,3',4-Pentachlorobiphenyl	CB 82	338	340	0.03
2,3',4,4',5-Pentachlorobiphenyl	CB 118	326	328	0.03
2,3,4,4',5-Pentachlorobiphenyl	CB 114	326	328	0.02
2,2',4,4',5,5'-Hexachlorobiphenyl	CB 153	360	362	0.02
2,3,3',4,4'-Pentachlorobiphenyl	CB 105	326	324	0.02
2,2',3,3',5,6,6'-Heptachlorobiphenyl	CB 179	396	398	0.03
2,2',3,4,4',5'-Hexachlorobiphenyl	CB 138	360	362	0.02
2,3,3',4,4',6-Hexachlorobiphenyl	CB 158	326	328	0.03
3,3',4,4',5-Pentachlorobiphenyl	CB 126	360	362	0.02
2,3,4,4',5,6-Hexachlorobiphenyl	CB 166	394	396	0.02
2,2',3,4',5,5',6-Heptachlorobiphenyl	CB 187	394	396	0.02
2,2',3,4,4',5',6-Heptachlorobiphenyl	CB 183	360	362	0.02
2,2',3,3',4,4'-Hexachlorobiphenyl	CB 128	360	362	0.02
2,3,3',4,4',5-Hexachlorobiphenyl	CB 156	360	362	0.02
2,2',3,4,4',5,5'-Heptachlorobiphenyl	CB 180	394	396	0.03
3,3',4,4',5,5'-Hexachlorobiphenyl	CB 169	360	362	0.03
2,2',3,3',4,4',5-Heptachlorobiphenyl	CB 170	394	396	0.03
2,3,3',4,4',5,5'-Heptachlorobiphenyl	CB 189	394	396	0.03
Polycyclic aromatic hydrocarbons (PAHs)				
Acenaphthylene	Acl	152	151	0.06
Acenaphthene	Ace	153	154	0.12
Fluorene	Flu	166	165	0.15
Phenanthrene	Phe	178	176	0.06
Anthracene	Ant	178	176	0.07
Fluoranthene	Fl	202	200	0.09
Pyrene	Py	202	200	0.12
11H-benzo[*a*]fluorene	11BaF	216	215	0.04
11H-benzo[*b*]fluorene	11BbF	216	215	0.04
Benzo[*b*]naphtho[*2,3-d*]furan	BBNF	218	189	0.32
Benzo[*a*]anthracene	BaA	228	226	0.06
Chrysene	Chr	228	226	0.03
Benzo[*b*]naphtho[*2,1-d*]thiophene	BBNT	234	235	0.12
4,5-Methanochrysene	4,5MC	239	240	2.0
5-Methylbenzo[*a*]anthracene	5MBA	242	241	0.20
1-Methylchrysene	1MC	242	241	0.14

7-Methylbenz[*a*]anthracene	7MbA	242	241	0.09
Benzo[*b*]fluoranthene	BbF	252	253	0.08
Benzo[*k*]fluoranthene	BkF	252	253	0.20
Benzo[*j*]fluoranthene	BjF	252	253	0.52
Benzo[*a*]pyrene	BaP	252	253	0.09
Perylene	Pery	252	264	0.23
7,12-Dimethylbenz[*a*]anthracene	7,12DbA	256	241	0.05
10-Methylbenzo[*a*]pyrene	10MbA	266	256	0.32
20-Methylcholanthrene	20Mc	268	252	0.12
Indeno[*1,2,3-cd*]pyrene	IcdP	276	138	0.09
Benzo[*g,h,i*]perylene	BghiP	276	138	0.12
Dibenz[*a,h*]anthracene	DbahA	278	276	0.07
Alkylated PAHs (alkyl-PAHs)				
1-Methylnaphthalene	1-Na	142	141	
2-Methylnaphthalene	2-Na	142	141	
1,3-Dimethylnaphthalene	1,3-Na	156	141	
1,4,5-Trimethylnaphthalene	1,4,5-Na	170	155	
1,2,5,6-Tetramethylnaphthalene	1,2,5,6-Na	184	169	
1-Methylfluorene	1-Flu	180	165	
9-Methylfluorene	9-Flu	180	165	
Dibenzothiophene	Dbthio	184	185	
2-Methyldibenzothiophene	2-Dbthio	198	197	
2,4-Dimethyldibenzothiophene	2,4-Dbthio	212	197	
2,4,7-Trimethyldibenzothiophene	2,4,7-Dbthio	226	211	
3-Methylphenanthrene	3-Phe	192	191	
2-Methylphenanthrene	2-Phe	192	191	
1,6-Dimethylphenanthrene	1,6-Phe	206	191	
1,2-Dimethylphenanthrene	1,2-Phe	206	191	
1,2,9-Trimethylphenanthrene	1,2,9-Phe	220	-	
1,2,6,9-Tetramethylphenanthrene	1,2,6,9-Phe	234	219	
3-Methylchrysene	3-Chr	242	239	
6-Ethylchrysene	6-Ethyl-Chr	256	241	
1,3,6-Trimethylchrysene	1,3,6-Chr	252	264	
Internal standard				
2-Fluorobiphenyl	IS	172	171	
Surrogate standards		**Quantification ion**	**Confirmation ion**	**Surrogate recovery (%, mean ± SD)**
Polychlorinated biphenyls (PCBs)				
^{13}C-labeled CB 28		268	270	80 ± 18
^{13}C-labeled CB 52		304	302	99 ± 6
^{13}C-labeled CB 101		326	328	84 ± 18
^{13}C-labeled CB 153		372	374	109 ± 7
^{13}C-labeled CB 138		360	362	90 ± 6
^{13}C-labeled CB 180		406	408	94 ± 7
^{13}C-labeled CB 209		510	512	92 ± 8
Polycyclic aromatic hydrocarbons (PAHs)				
Acenaphthene-d10	Ace-d10	164	162	83 ± 6
Phenanthrene-d10	Phe-d10	188	189	98 ± 11
Chrysene-d12	Chr-d12	240	236	94 ± 20

Table S3. Instrumental conditions of GC-MSD for PCBs, PAHs, and alkyl-PAHs analyses.

Instrument	GC: Agilent Technologies 7890B, MSD: Agilent Technologies 5977B	
Analytical column	DB-5MS (30 m × 0.25 mm i.d. × 0.25 μm film)	
Carrier gas	Helium	
Flow rate	1.0 mL min^{-1}	
Injection volume	1.0 μL	
Mass range	50–600 *m/z*	
Ion source temperature	230 ℃	
Ionization mode	EI mode (70 eV)	
Oven temperature	PCBs	60 ℃ (hold 1 min) →
		5 ℃ min^{-1} to 140 ℃ (hold 1 min) →
		30 ℃ min^{-1} to 200 ℃ (hold 1 min) →
		4 ℃ min^{-1} to 250 ℃ (hold 5 min) →
		10 ℃ min^{-1} to 300 ℃ (hold 1 min)
	PAHs	60 ℃ (hold 2 min) →
		6 ℃ min^{-1} to 300 ℃ (hold 13 min)
	Alkyl-PAHs	60 ℃ (hold 2 min) →
		6 ℃ min^{-1} to 162 ℃ (hold 0 min) →
		2 ℃ min^{-1} to 168 ℃ (hold 0 min) →
		6 ℃ min^{-1} to 300 ℃ (hold 13 min)

Table S4. Concentrations of polychlorinated biphenyls (PCBs) in soil samples from the glacier foreland of Midtre Lovénbreen, Svalbard.

Samples	Concentrations of PCBs (ng g^{-1} dw)								
	CB 8	CB 28	CB 37	CB 52	CB 49	CB 44	CB 74	CB 70	CB 66
ML 6	0.10	0.03	ND	0.09	0.22	0.26	0.02	0.02	ND
ML 204	0.08	ND	ND	0.04	0.23	0.30	ND	0.01	ND
ML 263	0.01	0.03	0.08	0.04	0.09	ND	ND	ND	ND
ML 66	0.03	ND	ND	0.06	0.08	0.09	ND	0.01	ND
ML 10	0.01	ND	ND	0.09	0.13	0.10	0.02	ND	ND
ML 177	0.02	ND	ND	0.06	0.16	0.15	ND	0.01	ND
ML 71	0.04	0.05	ND	0.08	0.08	0.05	ND	0.01	0.04
ML 20	0.04	ND	ND	0.06	0.11	0.13	0.02	0.01	ND
ML 25	0.03	0.03	ND	0.07	0.10	0.16	ND	ND	ND
ML 37	0.03	0.03	ND	0.07	0.08	0.04	ND	0.02	ND
ML 298	0.03	ND	ND	0.03	0.07	0.10	ND	0.01	ND
ML 47	0.10	ND	ND	0.09	0.14	0.08	0.02	0.03	ND
ML 130	0.01	ND	ND	0.03	0.12	ND	ND	0.01	ND
ML 62	0.04	ND	ND	0.05	0.11	0.06	0.02	ND	ND
ML 279	0.02	ND	ND	ND	0.06	0.07	0.03	0.02	ND
ML 60	0.08	ND	ND	0.03	0.09	0.05	0.05	0.02	ND
ML 102	0.04	ND	ND	0.10	0.21	0.18	ND	0.03	ND
ML 149	0.02	0.03	ND	0.06	0.06	0.05	0.02	0.01	ND
ML 81	0.07	ND	ND	0.03	0.06	0.10	ND	ND	ND
ML 84	0.02	0.04	ND	0.09	0.12	0.20	ND	0.03	ND
ML 141	0.02	ND	0.04	0.05	0.09	0.15	ND	ND	ND
ML 103	0.04	ND	ND	0.08	0.15	0.22	0.02	ND	ND
ML 222	0.07	ND	ND	0.06	0.15	0.14	ND	ND	ND
ML 93	0.01	ND	ND	ND	0.08	0.12	ND	ND	ND
ML 120	0.06	ND	ND	0.12	0.15	0.27	ND	0.02	0.03
ML 132	0.08	0.03	ND	0.05	0.14	0.10	ND	ND	ND
ML 231	0.05	ND	ND	0.06	0.09	0.12	ND	ND	ND
ML 253	0.01	ND	ND	0.07	0.08	0.06	ND	0.01	ND
ML 124	0.06	ND	ND	0.05	0.04	ND	ND	ND	ND
ML 266	0.02	ND	0.02	ND	0.09	0.07	ND	ND	ND
ML 138	0.04	ND	0.04	0.07	0.08	0.17	ND	ND	ND
ML 252	0.01	ND	0.03	0.05	0.08	ND	ND	ND	ND
ML 157	0.03	ND	ND	0.06	0.08	0.08	ND	ND	ND
ML 182	0.06	ND	ND	0.05	0.09	0.08	ND	ND	ND
ML 292	0.03	ND	ND	0.03	0.10	0.14	ND	ND	ND
ML 225	0.04	ND	ND	0.05	0.07	0.10	ND	ND	ND
ML 274	0.02	ND	ND	0.07	0.13	0.10	ND	0.01	ND
ML 191	0.02	ND	ND	0.06	0.11	0.16	ND	0.02	ND
ML 170	0.01	ND	0.02	0.04	0.08	0.06	0.03	0.03	0.03
ML 237	0.06	ND	ND	0.05	0.12	0.09	ND	ND	ND
ML 287	0.02	ND	ND	0.04	0.09	0.10	ND	ND	ND
ML 245	0.01	ND	ND	0.03	0.04	ND	0.03	ND	ND
ML 302	0.01	ND	ND	ND	0.03	0.03	ND	ND	ND
ML 301	0.03	ND	ND	ND	0.004	ND	ND	ND	ND
ML 303	ND[a]	ND	ND	ND	ND	ND	ND	0.01	ND

Table S4. (Continued).

Samples	Concentrations of PCBs (ng g^{-1} dw)								
	CB 60	**CB 77**	**CB 101**	**CB 99**	**CB 87**	**CB 82**	**CB 118**	**CB 114**	**CB 105**
ML 6	ND	ND	0.04	ND	0.02	ND	ND	ND	ND
ML 204	0.03	0.03	0.06	ND	0.04	ND	ND	ND	ND
ML 263	ND	0.02	0.05	ND	ND	ND	ND	ND	ND
ML 66	0.03	ND	0.02	ND	ND	0.04	ND	ND	ND
ML 10	ND	ND	0.02	ND	ND	ND	ND	ND	ND
ML 177	0.04	0.02	ND	ND	ND	ND	ND	ND	0.02
ML 71	0.05	0.03	0.03	ND	ND	ND	ND	ND	0.03
ML 20	ND	0.02	0.02	ND	ND	ND	ND	ND	ND
ML 25	ND	ND	ND	ND	ND	ND	ND	ND	ND
ML 37	0.05	0.03	ND	ND	ND	ND	ND	ND	ND
ML 298	ND	0.02	ND	ND	ND	0.03	ND	ND	ND
ML 47	0.04	0.04	0.05	ND	0.02	ND	ND	ND	ND
ML 130	ND	0.01	0.02	ND	ND	0.07	ND	ND	ND
ML 62	ND	0.02	0.03	0.05	ND	ND	ND	ND	0.02
ML 279	0.03	ND	ND	ND	ND	ND	ND	ND	ND
ML 60	ND	0.02	ND	0.03	ND	ND	ND	ND	ND
ML 102	0.04	0.02	0.05	ND	0.02	ND	ND	ND	0.06
ML 149	0.04	0.03	0.03	ND	ND	ND	ND	ND	ND
ML 81	ND	ND	ND	ND	ND	ND	ND	ND	ND
ML 84	ND	ND	ND	ND	ND	0.03	ND	ND	ND
ML 141	ND	ND	0.02	ND	ND	ND	ND	ND	0.03
ML 103	ND	0.06	0.03	ND	ND	ND	ND	ND	ND
ML 222	ND	0.02	ND	ND	ND	ND	ND	ND	ND
ML 93	ND	0.03	0.03	ND	ND	ND	ND	ND	ND
ML 120	ND	0.02	0.05	ND	0.02	ND	ND	0.02	ND
ML 132	0.03	ND	ND	ND	ND	ND	ND	ND	ND
ML 231	ND	0.02	ND	ND	ND	ND	0.03	0.04	ND
ML 253	ND	ND	ND	ND	ND	ND	ND	0.02	0.02
ML 124	ND	0.02	0.03	ND	ND	0.08	ND	ND	ND
ML 266	ND	0.03	0.04	ND	ND	ND	ND	0.02	ND
ML 138	0.04	ND	ND	ND	ND	ND	ND	ND	ND
ML 252	ND	ND	0.05	ND	0.02	ND	ND	ND	ND
ML 157	ND	0.02	0.02	ND	ND	ND	ND	0.02	0.04
ML 182	ND	0.02	0.06	ND	ND	ND	ND	ND	ND
ML 292	ND	ND	0.03	ND	ND	ND	ND	0.04	ND
ML 225	ND	0.01	ND	ND	ND	ND	ND	ND	ND
ML 274	ND	0.03	ND	ND	ND	ND	ND	0.02	ND
ML 191	ND	0.03	ND	ND	ND	ND	ND	0.03	ND
ML 170	ND	0.01	0.07	ND	ND	ND	ND	ND	0.03
ML 237	ND	0.02	ND	ND	ND	ND	ND	0.03	ND
ML 287	ND	0.01	0.03	ND	ND	ND	ND	ND	ND
ML 245	ND	0.01	0.03	ND	ND	ND	ND	ND	ND
ML 302	ND	0.02	0.04	ND	ND	ND	ND	ND	ND
ML 301	ND	0.02	ND	ND	ND	ND	ND	ND	ND
ML 303	ND	0.02	ND	ND	ND	ND	ND	0.03	ND

Table S4. (Continued).

Samples	Concentrations of PCBs (ng g^{-1} dw)								
	CB 126	**CB 153**	**CB 138**	**CB 158**	**CB 166**	**CB 128**	**CB 156**	**CB 169**	**CB 179**
ML 6	0.06	0.02	ND	ND	ND	0.02	ND	0.03	ND
ML 204	0.03	ND	ND	ND	ND	0.02	0.06	0.04	ND
ML 263	0.09	ND	ND	ND	ND	0.02	0.11	0.03	ND
ML 66	0.03	ND	ND	ND	0.05	ND	ND	ND	ND
ML 10	0.06	0.04	ND	ND	ND	0.03	0.05	ND	ND
ML 177	ND	ND	ND	ND	ND	ND	0.03	ND	ND
ML 71	0.06	0.02	ND	ND	0.04	ND	0.08	0.04	ND
ML 20	0.06	0.03	ND	ND	ND	0.07	0.02	ND	ND
ML 25	0.06	ND	ND	ND	ND	ND	0.03	ND	ND
ML 37	0.04	ND	ND	ND	0.09	ND	0.11	0.05	ND
ML 298	ND	ND	ND	ND	ND	ND	0.08	ND	ND
ML 47	ND	ND	ND	ND	ND	ND	0.02	0.04	ND
ML 130	ND	ND	ND	ND	0.05	ND	ND	ND	ND
ML 62	0.05	ND	ND	ND	0.03	ND	ND	ND	ND
ML 279	0.04	0.03	0.03	ND	0.04	0.03	ND	ND	ND
ML 60	0.05	0.02	ND	ND	ND	ND	0.06	ND	ND
ML 102	0.06	ND	ND	ND	ND	0.02	0.03	0.04	ND
ML 149	0.04	ND	ND	ND	ND	ND	ND	ND	ND
ML 81	0.09	ND	ND	ND	ND	ND	ND	ND	ND
ML 84	0.03	ND	ND	ND	0.03	ND	0.06	ND	ND
ML 141	ND	ND	ND	ND	0.05	ND	ND	ND	ND
ML 103	ND	ND	ND	ND	ND	ND	0.07	0.04	ND
ML 222	0.06	ND	ND	ND	ND	ND	0.04	ND	ND
ML 93	0.08	0.02	ND	ND	ND	0.03	0.03	ND	ND
ML 120	0.05	0.03	ND	ND	0.03	ND	ND	0.04	ND
ML 132	ND	0.03	0.02	ND	ND	0.02	ND	ND	ND
ML 231	0.06	ND	ND	ND	ND	0.06	0.05	ND	ND
ML 253	0.06	ND	ND	ND	ND	0.04	ND	ND	ND
ML 124	ND	ND	ND	ND	0.05	0.03	0.08	ND	ND
ML 266	ND	ND	ND	ND	ND	ND	0.05	ND	ND
ML 138	ND	ND	ND	ND	0.03	ND	0.04	ND	ND
ML 252	0.05	ND	ND	ND	ND	ND	ND	ND	ND
ML 157	0.13	ND	ND	ND	ND	0.03	ND	ND	ND
ML 182	0.05	ND	ND	ND	ND	ND	ND	ND	ND
ML 292	0.05	0.03	ND	ND	ND	ND	ND	ND	ND
ML 225	0.06	0.02	ND	ND	ND	0.02	0.03	ND	ND
ML 274	ND	0.02	ND	ND	0.04	ND	0.03	ND	ND
ML 191	0.04	0.04	ND	ND	ND	ND	ND	ND	ND
ML 170	0.05	ND	ND	ND	ND	ND	ND	ND	ND
ML 237	0.05	0.03	ND	ND	ND	0.04	ND	ND	ND
ML 287	ND	ND	ND	ND	ND	ND	0.02	ND	ND
ML 245	ND	0.03	ND	ND	0.02	0.04	0.06	ND	ND
ML 302	0.07	0.03	ND	ND	ND	ND	0.05	ND	ND
ML 301	0.04	ND	ND	ND	ND	0.04	0.08	ND	ND
ML 303	ND	0.02	0.02	ND	ND	0.03	0.03	ND	ND

Table S4. (Continued).

Samples	Concentrations of PCBs (ng g^{-1} dw)					
	CB 187	**CB 183**	**CB 180**	**CB 170**	**CB 189**	**SUM**
ML 6	ND	ND	ND	ND	0.04	0.97
ML 204	0.05	ND	0.04	ND	ND	1.07
ML 263	0.03	0.03	0.06	ND	ND	0.68
ML 66	0.05	0.11	0.06	ND	ND	0.65
ML 10	ND	ND	ND	ND	ND	0.56
ML 177	ND	ND	ND	ND	ND	0.51
ML 71	ND	ND	ND	ND	ND	0.73
ML 20	ND	ND	ND	ND	ND	0.61
ML 25	ND	ND	ND	ND	ND	0.49
ML 37	ND	ND	ND	ND	ND	0.63
ML 298	ND	ND	ND	ND	ND	0.37
ML 47	ND	ND	ND	ND	0.05	0.73
ML 130	ND	0.02	0.06	ND	0.12	0.53
ML 62	ND	0.06	ND	ND	ND	0.54
ML 279	ND	ND	ND	ND	ND	0.39
ML 60	ND	ND	ND	ND	ND	0.50
ML 102	ND	ND	ND	ND	0.16	1.1
ML 149	ND	ND	ND	ND	ND	0.43
ML 81	ND	ND	ND	ND	ND	0.35
ML 84	ND	ND	ND	ND	ND	0.66
ML 141	0.08	0.04	0.04	ND	ND	0.60
ML 103	0.08	0.03	ND	ND	ND	0.82
ML 222	0.16	0.12	ND	ND	ND	0.82
ML 93	ND	ND	ND	ND	ND	0.44
ML 120	0.06	ND	ND	ND	ND	0.97
ML 132	0.08	ND	ND	0.08	ND	0.67
ML 231	ND	ND	ND	ND	ND	0.57
ML 253	ND	0.15	0.12	ND	0.12	0.77
ML 124	0.07	0.09	ND	ND	ND	0.60
ML 266	ND	ND	ND	ND	ND	0.35
ML 138	0.02	ND	ND	0.04	ND	0.56
ML 252	0.03	ND	0.12	0.11	0.09	0.64
ML 157	ND	ND	ND	ND	ND	0.50
ML 182	ND	ND	ND	ND	ND	0.40
ML 292	ND	ND	ND	ND	ND	0.44
ML 225	ND	ND	ND	ND	ND	0.41
ML 274	ND	ND	ND	ND	ND	0.48
ML 191	ND	ND	ND	ND	ND	0.51
ML 170	ND	ND	ND	ND	ND	0.48
ML 237	ND	ND	ND	ND	ND	0.47
ML 287	ND	ND	ND	ND	ND	0.31
ML 245	ND	ND	ND	ND	ND	0.30
ML 302	0.03	ND	ND	ND	ND	0.30
ML 301	ND	ND	0.04	ND	ND	0.33
ML 303	0.04	ND	ND	ND	ND	0.25

[a] ND: Not detected.

Table S5. Concentrations of polycyclic aromatic hydrocarbons (PAHs) in soil samples from the glacier foreland of Midtre Lovénbreen, Svalbard.

Samples	Concentrations of PAHs (ng g^{-1} dw)									
	Acl	Ace	Flu	Phe	Ant	Fl	Py	11BaF	11BbF	BBNF
ML 6	1.7	3.9	5.1	27	2.0	3.8	4.7	3.2	0.75	3.0
ML 204	0.87	2.4	4.8	24	1.5	4.3	3.8	4.0	0.56	1.2
ML 263	0.64	1.8	3.7	13	1.2	2.5	2.0	3.0	0.27	0.43
ML 66	1.3	2.9	5.6	25	1.6	3.6	4.0	5.8	0.59	1.0
ML 10	0.95	2.4	5.6	17	0.89	4.5	3.6	3.7	0.48	0.55
ML 177	1.1	3.5	7.3	42	2.2	9.0	12	4.4	1.7	2.9
ML 71	1.2	3.1	5.5	27	2.0	4.1	4.7	4.4	0.90	1.1
ML 20	0.78	2.7	6.1	19	1.4	2.6	2.2	2.7	0.36	0.47
ML 25	0.78	2.7	5.6	20	1.1	2.9	3.2	2.7	0.50	0.68
ML 37	0.71	2.1	4.5	14	1.3	2.2	2.2	2.5	0.27	0.45
ML 298	0.36	1.6	4.4	11	0.49	1.8	1.4	0.59	0.08	ND[a]
ML 47	1.6	4.5	6.1	28	2.3	3.6	4.0	3.4	0.59	1.0
ML 130	0.25	1.4	2.5	9.4	0.92	1.2	1.1	0.11	0.06	ND
ML 62	0.27	1.6	3.4	9.3	0.19	1.2	1.2	0.25	0.09	ND
ML 279	0.28	1.1	2.7	7.8	0.49	1.5	1.2	0.49	0.07	ND
ML 60	1.2	3.2	3.7	24	1.9	3.3	3.6	4.0	0.62	1.1
ML 102	5.1	9.8	19	140	9.0	27	42	22	9.7	18
ML 149	0.24	1.3	3.2	7.2	0.49	0.97	0.78	0.08	0.04	ND
ML 81	1.1	2.6	5.1	24	1.7	4.2	4.8	3.6	0.74	1.2
ML 84	0.37	1.5	3.0	10	0.55	1.5	1.3	1.3	0.16	ND
ML 141	0.20	1.1	3.0	6.8	0.50	0.86	0.72	0.12	0.06	ND
ML 103	0.71	2.4	4.9	20	1.1	3.0	3.9	2.5	0.47	0.73
ML 222	1.8	4.6	10	68	4.1	15	18	7.1	3.1	5.6
ML 93	0.34	1.5	4.0	11	0.21	1.3	1.4	0.33	0.15	ND
ML 120	0.94	3.0	4.5	24	0.30	3.2	3.8	1.8	0.43	0.61
ML 132	1.3	3.3	5.2	30	1.3	3.7	4.1	2.4	0.82	1.1
ML 231	0.67	2.0	4.5	20	1.4	3.8	4.0	2.0	0.51	0.92
ML 253	0.70	1.8	3.3	12	0.84	1.8	1.6	3.6	0.20	0.38
ML 124	0.26	1.3	2.4	7.8	0.64	0.90	0.86	0.22	0.05	ND
ML 266	0.25	1.3	3.7	9.3	0.46	1.4	1.0	0.24	0.11	ND
ML 138	0.87	2.2	4.0	16	0.95	2.4	2.2	3.3	0.32	0.52
ML 252	0.56	1.6	3.0	15	0.48	1.9	1.5	0.57	0.18	0.47
ML 157	0.72	2.0	3.9	18	1.1	2.5	2.6	1.1	0.39	0.57
ML 182	1.4	3.7	5.5	32	1.6	4.3	4.6	2.1	0.87	1.3
ML 292	0.22	1.4	3.9	9.9	0.46	1.3	0.99	0.23	0.07	ND
ML 225	1.0	3.1	6.3	28	1.9	4.1	5.2	1.9	0.97	1.7
ML 274	1.2	2.8	4.3	26	1.5	3.4	4.1	1.8	0.73	1.3
ML 191	0.32	1.4	3.5	11	0.63	1.6	1.4	0.40	0.12	ND
ML 170	0.36	1.4	3.9	11	1.0	1.4	1.2	0.79	0.16	ND
ML 237	0.60	1.8	3.7	15	0.73	2.2	2.4	0.84	0.44	0.73
ML 287	0.16	1.1	3.3	7.6	0.57	1.2	1.0	0.17	ND[a]	ND
ML 245	0.54	1.7	3.0	15	1.1	2.1	2.4	0.40	0.27	0.47
ML 302	0.17	1.4	3.5	9.5	0.39	1.5	1.3	0.06	0.07	ND
ML 301	0.19	1.4	3.9	9.9	0.40	1.5	0.98	0.20	0.05	ND
ML 303	0.29	1.4	3.2	12	0.27	1.7	1.7	0.44	0.13	0.33

Table S5. (Continued).

Samples	Concentrations of PAHs (ng g^{-1} dw)									
	BaA	**Chr**	**BBNT**	**4,5MC**	**5MBA**	**1MC**	**7MbA**	**BbF**	**BkF**	**BjF**
ML 6	3.9	4.9	2.1	ND	0.61	0.70	0.23	3.6	2.9	1.9
ML 204	1.1	1.7	0.50	ND	0.29	0.46	ND	2.6	0.41	ND
ML 263	0.47	0.76	0.15	ND	ND	0.17	ND	1.8	1.3	ND
ML 66	0.88	1.2	0.24	ND	ND	0.52	ND	2.5	0.40	ND
ML 10	0.99	1.2	0.28	ND	ND	0.24	ND	3.7	0.94	0.81
ML 177	3.5	3.3	0.15	ND	0.81	0.67	ND	9.1	1.3	0.90
ML 71	1.1	1.4	0.14	ND	ND	0.35	ND	3.4	0.65	ND
ML 20	0.45	0.85	0.26	ND	ND	0.17	ND	1.3	0.24	ND
ML 25	0.88	1.1	0.23	ND	0.25	0.22	ND	2.3	0.53	ND
ML 37	0.52	0.49	0.16	ND	ND	0.17	ND	1.3	0.26	ND
ML 298	0.13	0.28	ND	ND	ND	ND	ND	0.49	ND	ND
ML 47	0.79	1.3	0.14	ND	ND	0.35	ND	1.9	1.3	ND
ML 130	0.07	0.27	ND	ND	ND	ND	ND	0.38	ND	ND
ML 62	0.16	0.35	ND	ND	ND	ND	ND	0.62	ND	ND
ML 279	0.10	0.33	ND	ND	ND	ND	ND	0.47	ND	ND
ML 60	0.85	1.2	0.19	ND	ND	0.30	ND	3.8	0.58	ND
ML 102	15	13	1.2	2.3	3.9	5.0	0.61	61	12	9.4
ML 149	0.09	0.38	ND	ND	ND	ND	ND	0.29	ND	ND
ML 81	0.88	1.1	0.15	ND	ND	0.54	ND	2.8	0.62	ND
ML 84	0.11	0.30	0.14	ND	ND	ND	ND	0.73	ND	ND
ML 141	0.08	0.16	ND	ND	ND	ND	ND	0.31	0.53	ND
ML 103	0.58	0.84	0.15	ND	ND	0.18	ND	1.9	0.30	ND
ML 222	5.3	5.5	0.39	ND	1.1	0.97	0.18	16	2.8	3.0
ML 93	0.15	0.26	0.20	ND	ND	ND	ND	0.68	ND	ND
ML 120	0.46	0.83	0.13	ND	ND	0.21	ND	1.6	0.32	ND
ML 132	0.86	1.5	0.19	ND	0.42	0.27	ND	1.7	0.42	ND
ML 231	0.85	1.1	0.17	ND	0.20	0.18	ND	2.9	1.2	0.70
ML 253	0.32	0.49	0.12	ND	ND	0.15	ND	0.66	0.34	ND
ML 124	0.08	0.10	ND	ND	ND	ND	ND	0.33	ND	ND
ML 266	0.12	0.40	ND	ND	ND	ND	ND	0.53	0.49	ND
ML 138	0.36	0.55	ND	ND	ND	0.18	ND	0.97	0.97	ND
ML 252	0.44	0.66	0.16	ND	ND	ND	ND	0.71	0.34	ND
ML 157	0.30	0.82	ND	ND	ND	ND	ND	1.2	0.57	ND
ML 182	0.87	1.3	0.14	ND	ND	0.23	ND	1.8	0.50	ND
ML 292	0.03	0.21	ND	ND	ND	ND	ND	0.35	0.21	ND
ML 225	1.5	1.4	0.23	ND	0.27	0.30	ND	2.9	0.89	0.53
ML 274	1.1	0.95	0.19	ND	0.53	0.49	ND	1.7	1.0	ND
ML 191	0.12	0.43	ND	ND	ND	ND	ND	0.59	ND	ND
ML 170	0.14	0.38	ND	ND	ND	ND	ND	12	37	12
ML 237	0.59	0.73	0.16	ND	ND	0.17	ND	1.2	0.31	ND
ML 287	0.09	0.12	ND	ND	ND	ND	ND	0.34	ND	ND
ML 245	0.48	0.67	0.14	ND	ND	ND	ND	0.72	0.62	ND
ML 302	0.13	0.21	0.12	ND	ND	ND	ND	0.56	0.37	ND
ML 301	0.09	0.33	ND	ND	ND	ND	ND	0.43	ND	ND
ML 303	0.26	0.29	ND	ND	ND	ND	ND	0.77	0.28	ND

Table S5. (Continued).

Samples	Concentrations of PAHs (ng g^{-1} dw)								
	BaP	Pery	7,12DbA	10MbA	20MC	IcdP	BghiP	DbahA	SUM[b]
ML 6	1.9	6.2	0.22	0.82	ND	3.3	3.6	7.3	93
ML 204	0.38	5.0	0.15	ND	ND	0.44	0.76	0.70	57
ML 263	0.39	1.6	0.06	ND	ND	0.17	0.40	0.10	34
ML 66	0.48	18	0.21	ND	ND	0.48	1.4	0.30	60
ML 10	0.49	5.3	0.15	ND	ND	0.42	0.75	0.36	50
ML 177	1.2	110	0.22	ND	ND	1.2	10	0.81	120
ML 71	0.47	1	0.16	ND	ND	0.56	2.5	0.35	66
ML 20	0.30	7.1	0.05	ND	0.13	0.21	0.67	0.36	44
ML 25	0.47	10	0.05	ND	ND	0.40	1.7	0.33	49
ML 37	0.27	6.1	0.06	ND	ND	0.22	0.64	0.19	35
ML 298	0.10	0.45	ND	ND	ND	ND	ND	ND	23
ML 47	0.34	12	0.12	ND	ND	0.28	2.0	0.21	63
ML 130	ND	4.8	ND	ND	ND	ND	0.16	ND	18
ML 62	0.09	9.1	ND	ND	ND	0.10	0.47	0.12	19
ML 279	ND	0.44	ND	ND	ND	ND	ND	ND	17
ML 60	0.44	7.4	0.28	ND	ND	0.39	1.8	ND	57
ML 102	11	670	3.5	2.1	1.2	14	96	10	570
ML 149	ND	1.6	ND	ND	ND	ND	ND	ND	15
ML 81	0.35	18	0.21	ND	ND	0.43	1.8	0.23	58
ML 84	0.20	1.5	ND	ND	ND	ND	0.27	0.07	22
ML 141	ND	1.6	ND	ND	ND	ND	ND	ND	14
ML 103	0.21	6.3	0.06	ND	ND	0.22	1.1	0.19	46
ML 222	2.3	110	0.50	1.1	0.18	2.5	20	2.7	200
ML 93	0.18	3.2	ND	ND	ND	0.09	0.21	ND	22
ML 120	0.31	13	ND	ND	ND	0.11	0.77	ND	47
ML 132	0.25	9.1	0.07	ND	ND	0.23	0.95	0.20	60
ML 231	0.51	14	0.16	ND	ND	0.25	1.2	0.34	50
ML 253	0.10	1.8	ND	ND	ND	ND	0.18	0.09	29
ML 124	ND	2.9	ND	ND	ND	ND	0.12	ND	15
ML 266	0.10	1.0	ND	ND	ND	ND	0.12	ND	20
ML 138	0.18	2.1	0.06	ND	ND	0.09	0.41	0.07	37
ML 252	0.16	2.6	ND	ND	ND	ND	0.30	0.13	28
ML 157	0.23	11	0.06	ND	ND	ND	0.55	ND	37
ML 182	0.21	8.1	0.12	ND	ND	0.12	0.88	0.14	64
ML 292	0.05	1.0	ND	ND	ND	ND	ND	ND	19
ML 225	0.37	35	0.11	ND	ND	0.48	3.3	0.65	67
ML 274	0.31	5.5	0.21	ND	ND	0.15	0.88	0.19	55
ML 191	0.10	1.0	ND	ND	ND	ND	0.15	ND	22
ML 170	0.10	2.9	0.31	ND	ND	0.09	0.33	ND	84
ML 237	0.26	6.4	0.05	ND	ND	0.17	0.58	0.17	32
ML 287	ND	1.2	ND	ND	ND	ND	0.08	ND	16
ML 245	0.11	1.8	ND	ND	ND	0.11	0.28	0.15	30
ML 302	0.09	1.6	ND	ND	ND	ND	0.15	ND	20
ML 301	0.22	1.3	ND	ND	ND	ND	0.14	ND	20
ML 303	0.09	5.8	ND	ND	ND	ND	0.28	ND	24

[a] ND: Not detected.

[b]: Sum of concentrations of PAHs except for perylene.

Table S6. Concentrations of alkyl-PAHs in soil samples from the glacier foreland of Midtre Lovénbreen, Svalbard.

Samples	Concentrations of alkyl-PAHs (ng g^{-1} dw)								
	C1-Na	C2-Na	C3-Na	C4-Na	C1-Flu	C2-Flu	Dbthio	C1-Dbthio	C2-Dbthio
ML 6	50	61	76	5.1	9.0	24	0.13	5.2	2.6
ML 204	22	33	48	3.6	4.7	9.1	0.09	4.1	1.9
ML 263	14	22	35	2.7	3.4	7.6	0.08	3.6	1.7
ML 66	38	64	93	6.9	5.7	12	0.20	7.3	2.9
ML 10	17	28	44	3.4	4.6	9.7	0.10	4.2	2.3
ML 177	59	61	69	5.5	8.0	11	0.15	6.0	2.1
ML 71	44	54	61	4.2	7.1	12	0.09	5.2	3.0
ML 20	24	31	42	3.1	3.9	9.2	0.11	4.2	2.3
ML 25	24	33	43	3.3	4.5	9.7	0.09	4.0	2.1
ML 37	16	27	45	3.6	4.2	9.6	0.08	3.8	1.8
ML 298	6.8	9.6	12	1.1	2.9	6.4	0.04	1.9	0.95
ML 47	43	57	78	5.5	9.8	32	0.18	6.2	3.3
ML 130	9.2	11	11	1.1	2.7	6.0	0.03	1.7	0.95
ML 62	9.1	11	12	1.2	2.9	7.3	0.05	1.8	1.4
ML 279	5.9	7.8	9.4	0.9	1.8	4.8	0.02	1.4	0.78
ML 60	41	53	63	4.3	5.0	11	0.15	5.6	3.8
ML 102	110	220	480	46	26	34	1.6	50	11
ML 149	5.3	5.3	5.4	0.7	2.2	5.0	0.02	1.2	0.60
ML 81	29	49	88	7.2	5.3	11	0.20	7.6	2.6
ML 84	8.3	13	19	1.6	2.9	7.6	0.04	2.4	1.4
ML 141	4.9	5.3	5.8	0.7	2.1	5.1	0.02	1.3	0.69
ML 103	21	29	38	2.9	4.7	9.6	0.09	4.0	2.3
ML 222	78	83	100	8.0	12	14	0.20	7.9	2.3
ML 93	9.1	12	15	1.4	3.2	7.8	0.04	2.4	1.5
ML 120	25	35	45	3.5	5.9	11	0.08	4.5	2.5
ML 132	55	63	62	3.9	5.4	9.9	0.11	4.8	3.1
ML 231	18	23	31	2.6	4.2	7.3	0.05	3.0	1.3
ML 253	18	28	42	3.0	3.1	7.0	0.06	3.7	1.3
ML 124	7.1	9.5	12	1.2	3.0	6.0	0.03	1.9	0.74
ML 266	6.4	7.6	7.5	0.8	2.4	5.2	0.02	1.3	0.88
ML 138	30	37	46	3.0	3.7	7.9	0.08	3.8	2.0
ML 252	27	24	19	1.3	2.6	6.0	0.04	2.3	1.8
ML 157	19	28	33	2.4	3.8	7.7	0.08	3.3	2.1
ML 182	71	71	66	4.0	5.7	10	0.11	5.2	4.1
ML 292	4.7	5.3	5.8	0.7	2.4	6.1	0.03	1.5	0.85
ML 225	41	41	49	4.1	6.1	8.7	0.03	4.3	1.9
ML 274	50	52	50	3.3	4.5	9.4	0.11	4.5	3.2
ML 191	9.3	11	13	1.1	2.7	6.0	0.04	1.7	1.0
ML 170	8.4	11	16	1.4	2.7	6.4	0.04	2.2	0.87
ML 237	22	23	25	1.9	3.5	7.0	0.04	2.6	1.9
ML 287	2.6	3.6	4.4	0.6	2.1	5.3	0.02	1.4	0.83
ML 245	16	19	20	1.6	3.1	7.7	0.04	2.3	1.5
ML 302	4.8	5.3	5.2	0.7	3.0	6.4	0.03	1.6	1.2
ML 301	5.2	5.9	6.0	0.8	2.5	6.5	0.02	1.4	1.1
ML 303	10	13	18	1.8	3.2	6.6	0.03	2.5	1.3

Table S6. (Continued).

Samples	Concentrations of alkyl-PAHs (ng g^{-1} dw)								
	C3-Dbthio	C1-Phe	C2-Phe	C3-Phe	C4-Phe	C1-Chr	C2-Chr	C3-Chr	SUM
ML 6	1.0	28	42	64	98	5.1	25	45	540
ML 204	0.87	16	21	54	90	5.9	33	8.9	360
ML 263	1.3	10	15	46	80	2.9	22	7.0	270
ML 66	1.4	23	31	82	140	7.6	43	13	570
ML 10	1.1	14	20	60	150	5.2	32	9.2	400
ML 177	1.0	22	24	42	34	11	31	8.6	400
ML 71	1.9	19	23	55	66	6.6	30	12	400
ML 20	1.1	12	16	48	100	3.8	24	6.8	340
ML 25	1.4	14	18	47	67	4.8	24	7.2	310
ML 37	0.84	10	15	43	62	3.1	20	6.9	270
ML 298	0.49	3.5	5.5	19	18	1.2	6.8	2.3	98
ML 47	1.7	37	64	93	89	5.3	23	57	600
ML 130	0.43	3.7	5.2	14	5.0	1.9	7.3	2.1	82
ML 62	0.69	3.6	5.6	17	4.8	2.0	9.2	3.0	92
ML 279	0.44	3.0	4.5	15	14	1.1	6.7	1.9	79
ML 60	1.9	23	27	69	110	8.5	40	11	480
ML 102	3.8	110	130	220	330	50	150	50	2000
ML 149	0.37	1.5	2.6	8.8	1.0	0.78	3.8	1.1	46
ML 81	1.2	21	27	63	100	6.5	32	9.4	460
ML 84	0.72	5.9	9.1	29	36	2.0	13	4.1	160
ML 141	0.35	1.9	3.1	9.6	2.0	0.90	4.0	1.0	49
ML 103	1.2	12	16	35	42	3.6	17	6.5	240
ML 222	1.2	31	33	64	69	17	49	14	580
ML 93	0.63	3.7	6.2	18	5.7	1.7	8.6	2.7	100
ML 120	1.2	16	19	49	61	6.2	28	9.7	320
ML 132	1.9	21	21	38	33	7.5	24	7.6	360
ML 231	0.50	10	12	33	45	4.1	21	6.8	220
ML 253	0.83	11	16	53	100	3.0	25	7.9	320
ML 124	0.31	3.1	4.5	14	8.3	1.5	6.1	2.1	81
ML 266	0.49	2.4	3.5	11	4.2	1.1	4.9	1.6	62
ML 138	1.0	14	17	50	83	3.8	22	6.7	330
ML 252	0.99	7.8	8.2	18	11	2.6	9.2	2.7	140
ML 157	1.2	9.8	11	23	17	3.9	14	4.3	180
ML 182	2.3	22	22	39	29	7.3	20	6.6	380
ML 292	0.56	2.2	3.7	13	4.5	0.85	5.2	1.6	59
ML 225	0.91	13	14	26	23	5.2	17	5.4	260
ML 274	2.0	17	20	43	22	8.1	22	9.3	320
ML 191	0.45	4.1	6.0	14	7.7	2.0	7.2	2.2	90
ML 170	0.40	4.1	5.9	18	18	1.7	20	3.3	120
ML 237	1.0	6.8	8.1	19	8.8	2.9	9.6	3.7	150
ML 287	0.44	1.7	3.3	11	4.0	0.73	3.9	1.4	48
ML 245	0.77	7.8	9.4	20	9.9	2.8	9.2	4.1	140
ML 302	0.65	1.8	3.4	11	2.1	1.1	3.9	1.4	54
ML 301	0.63	2.2	3.8	12	5.0	1.0	6.3	2.2	63
ML 303	0.56	4.0	6.6	17	8.4	1.8	7.6	1.8	100

Supplementary Figures

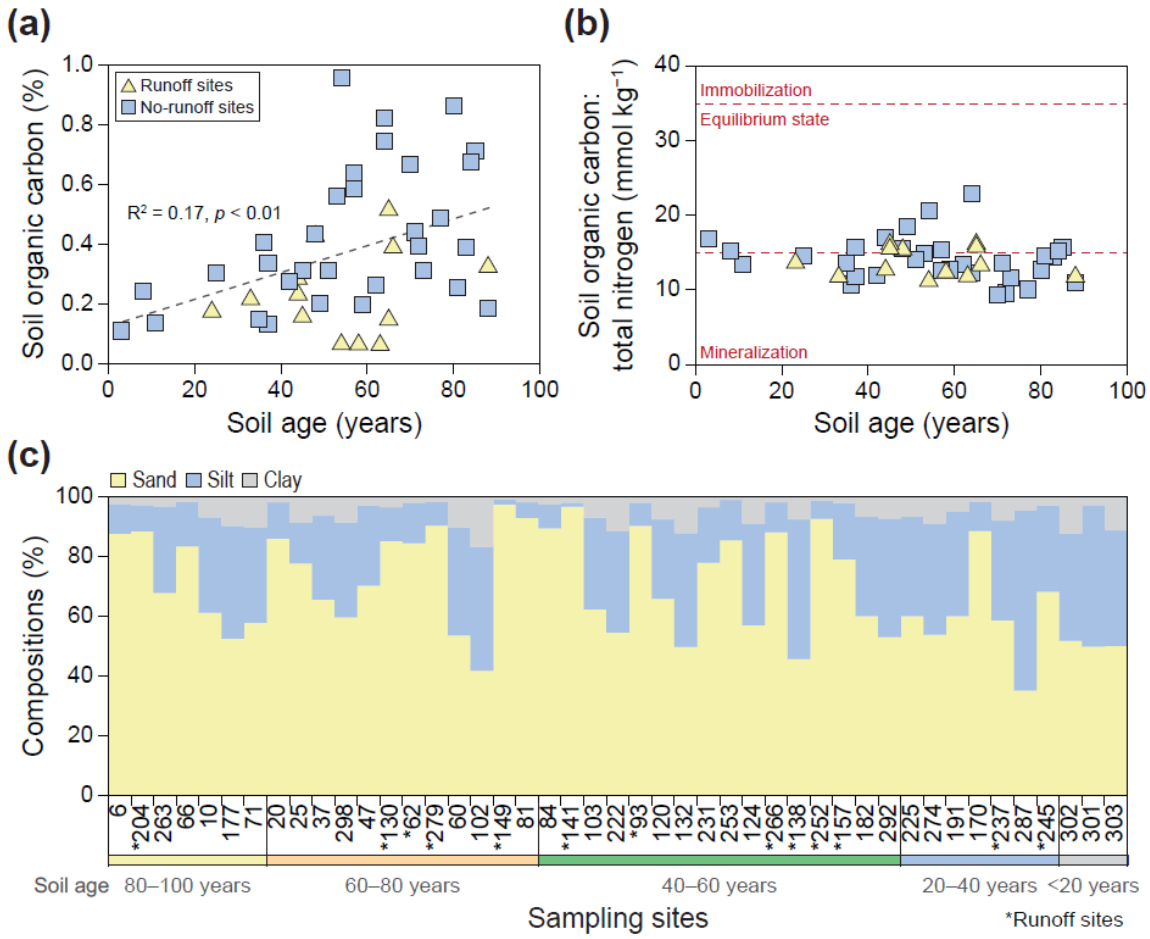

Fig. S1. (a) Correlation between soil organic carbon content (%) and soil age, **(b)** the ratio of soil organic carbon to total nitrogen associated with soil age, and **(c)** the relative composition of sand, silt, and clay in soils from the glacier foreland of Midtre Lovénbreen, Svalbard. Data for soil organic carbon, total nitrogen, and grain size were reported in a previous study (Kim et al., 2022).

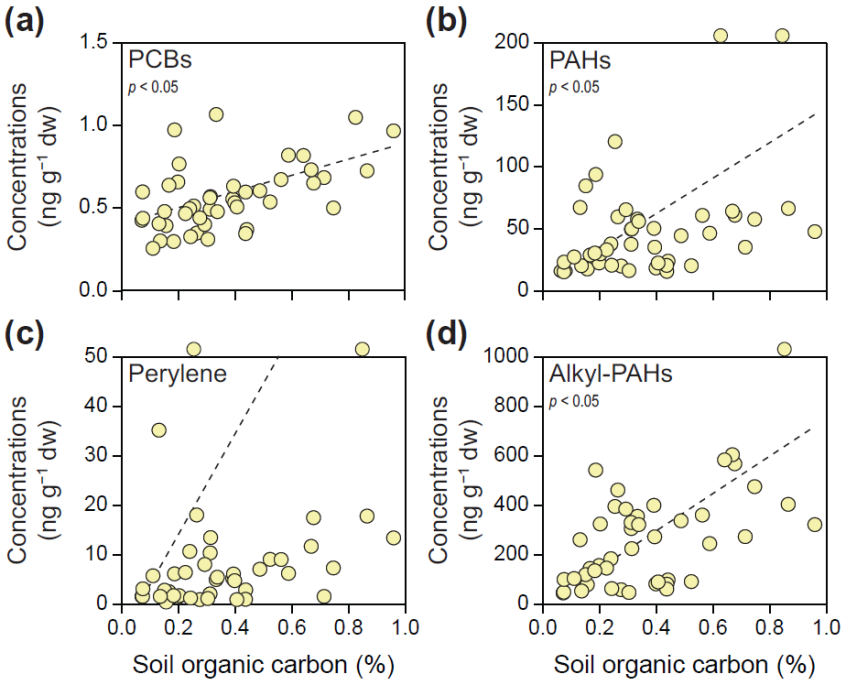

Fig. S2. Correlations between soil organic carbon content (%) and **(a)** PCBs, **(b)** PAHs, **(c)** perylene, and **(d)** alkyl-PAHs in soil samples from the glacier foreland of Midtre Lovénbreen, Svalbard. Data for soil organic carbon were reported in a previous study (Kim et al., 2022).

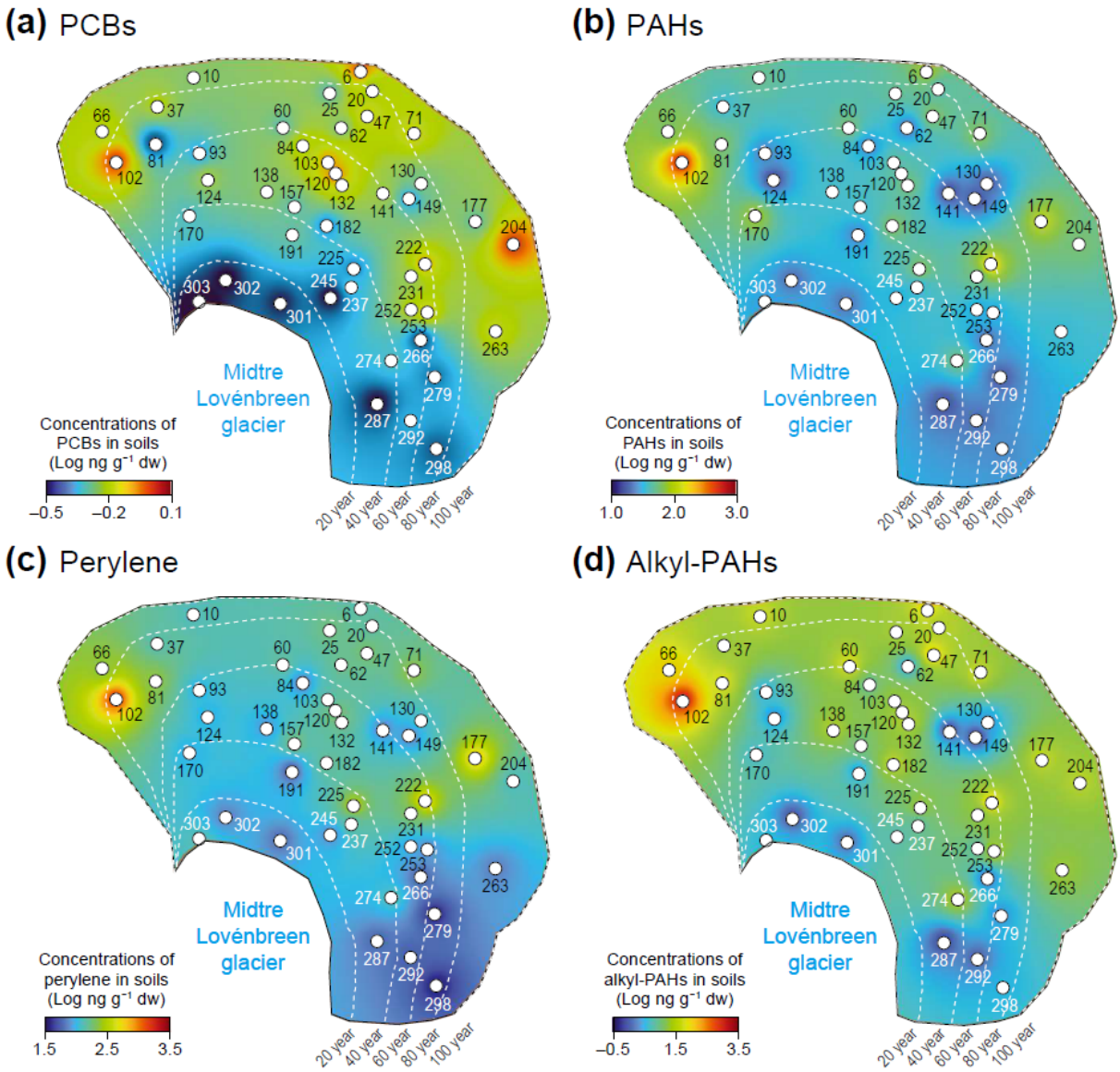

Fig. S3. Spatial distribution of **(a)** PCBs, **(b)** PAHs, **(c)** perylene, and **(d)** alkyl-PAHs in soil samples from the glacier foreland of Midtre Lovénbreen, Svalbard. The spatial distribution of PTSs in soils was estimated using qGIS software. The concentrations of the detected compounds are represented on a logarithmic scale.

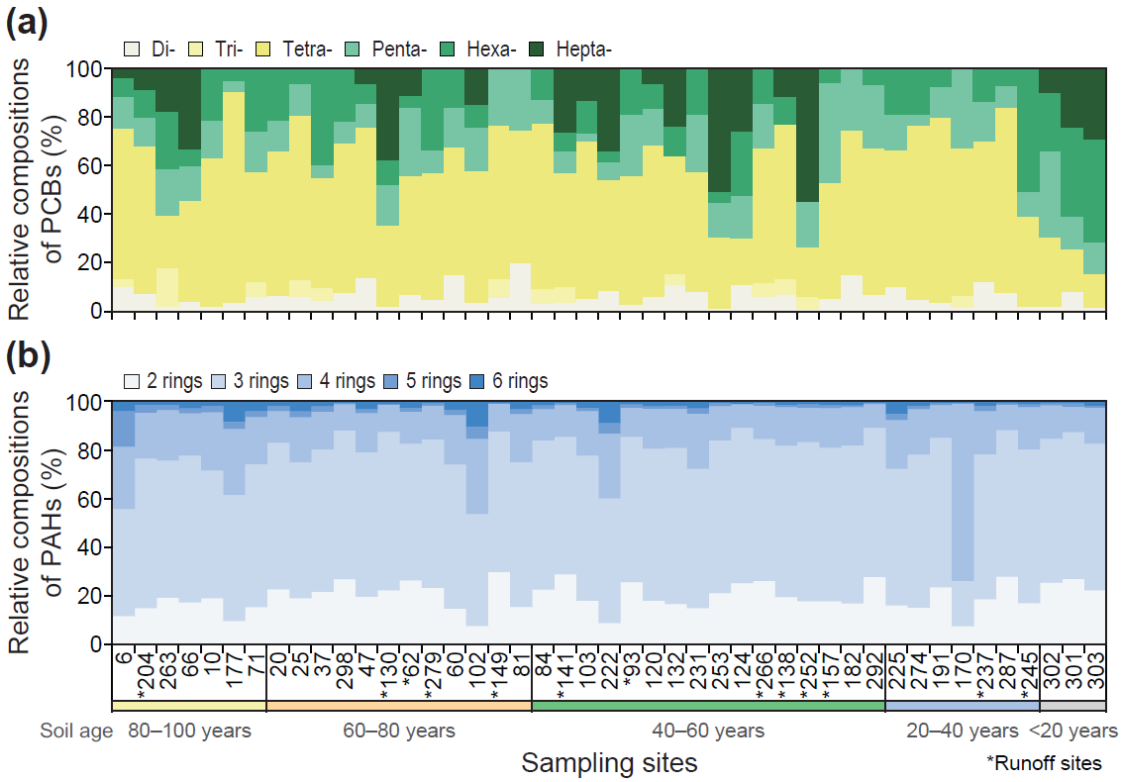

Fig. S4. Relative compositions of **(a)** PCBs and **(b)** PAHs in soil samples from the glacier foreland of Midtre Lovénbreen, Svalbard.

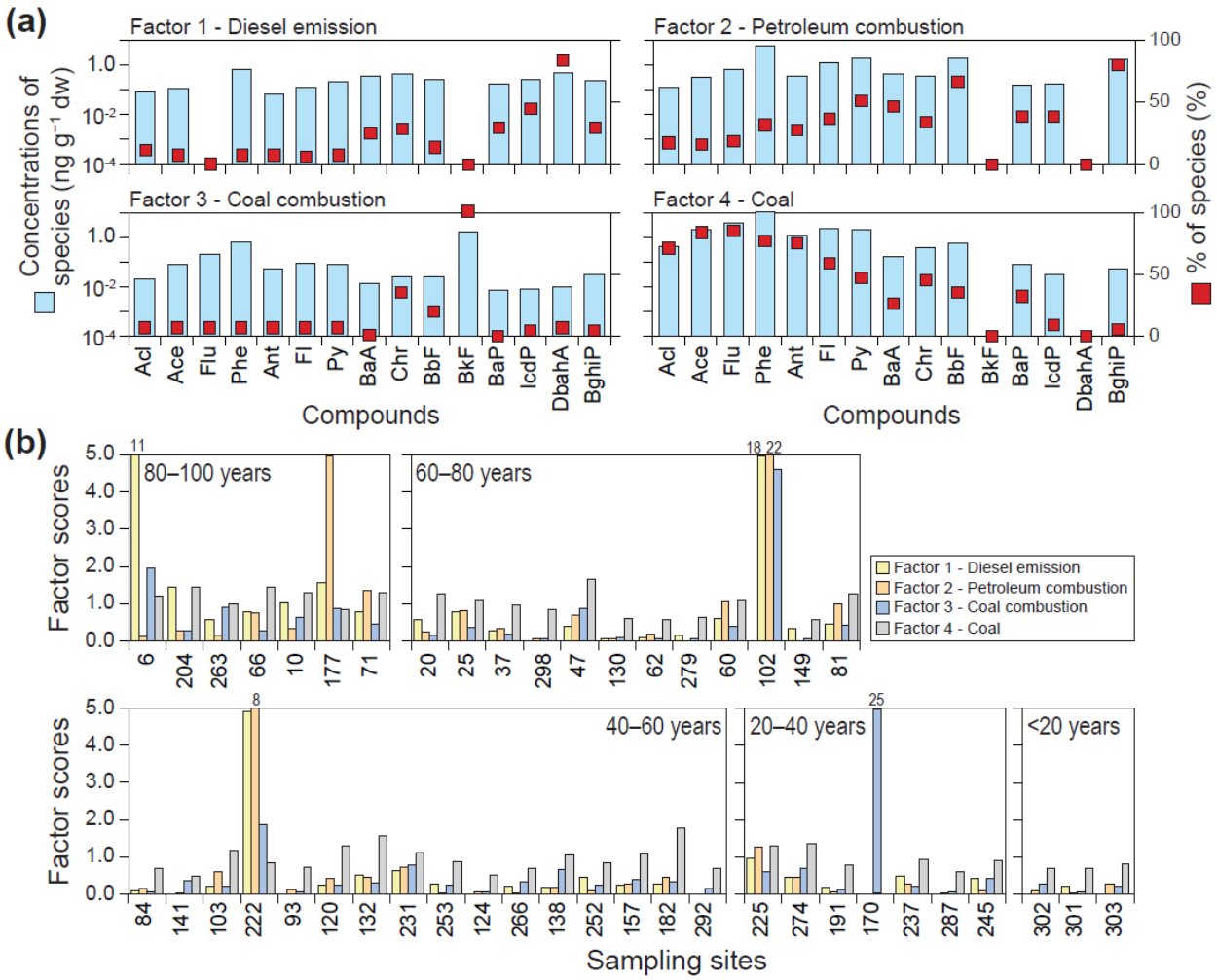

Fig. S5. (a) Source factors (Factor 1: diesel emission, Factor 2: petroleum combustion, Factor 3: coal combustion, and Factor 4: coal) estimated using the positive matrix factorization (PMF) model for PAHs in soil samples from the glacier foreland of Midtre Lovénbreen, Svalbard. **(b)** Contributions of each source to PAHs in the soil samples.

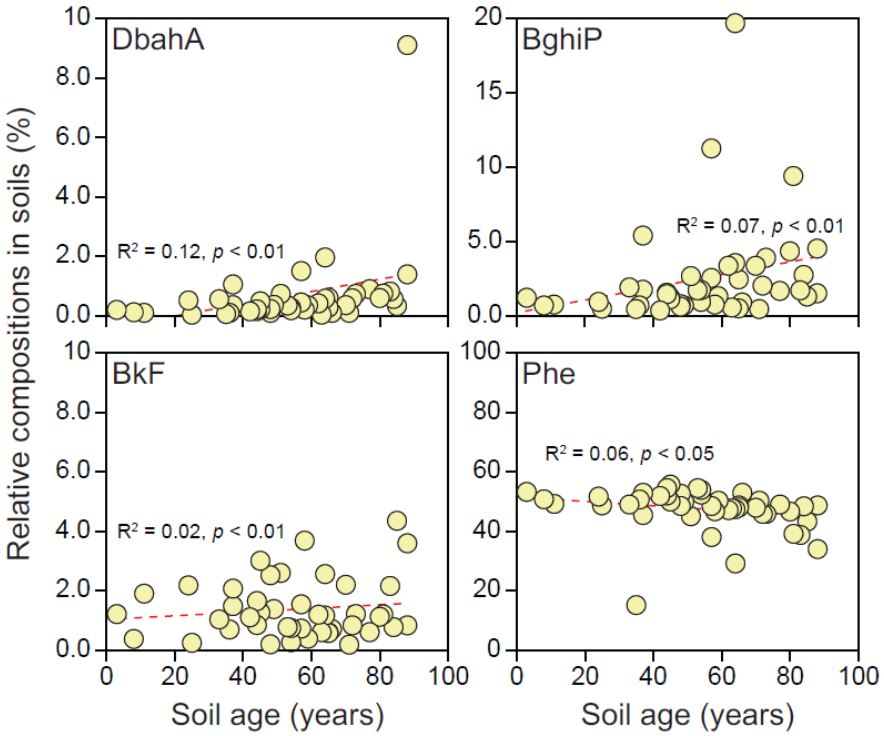

Fig. S6. Relative contributions of dibenz[*a,h*]anthracene (DbahA), benzo[*g,h,i*]perylene (BghiP), benzo[*k*]fluoranthene (BkF), and phenanthrene (Phe) to soil age. Data for the ML170 site in the soil were excluded due to their influence on result interpretation.

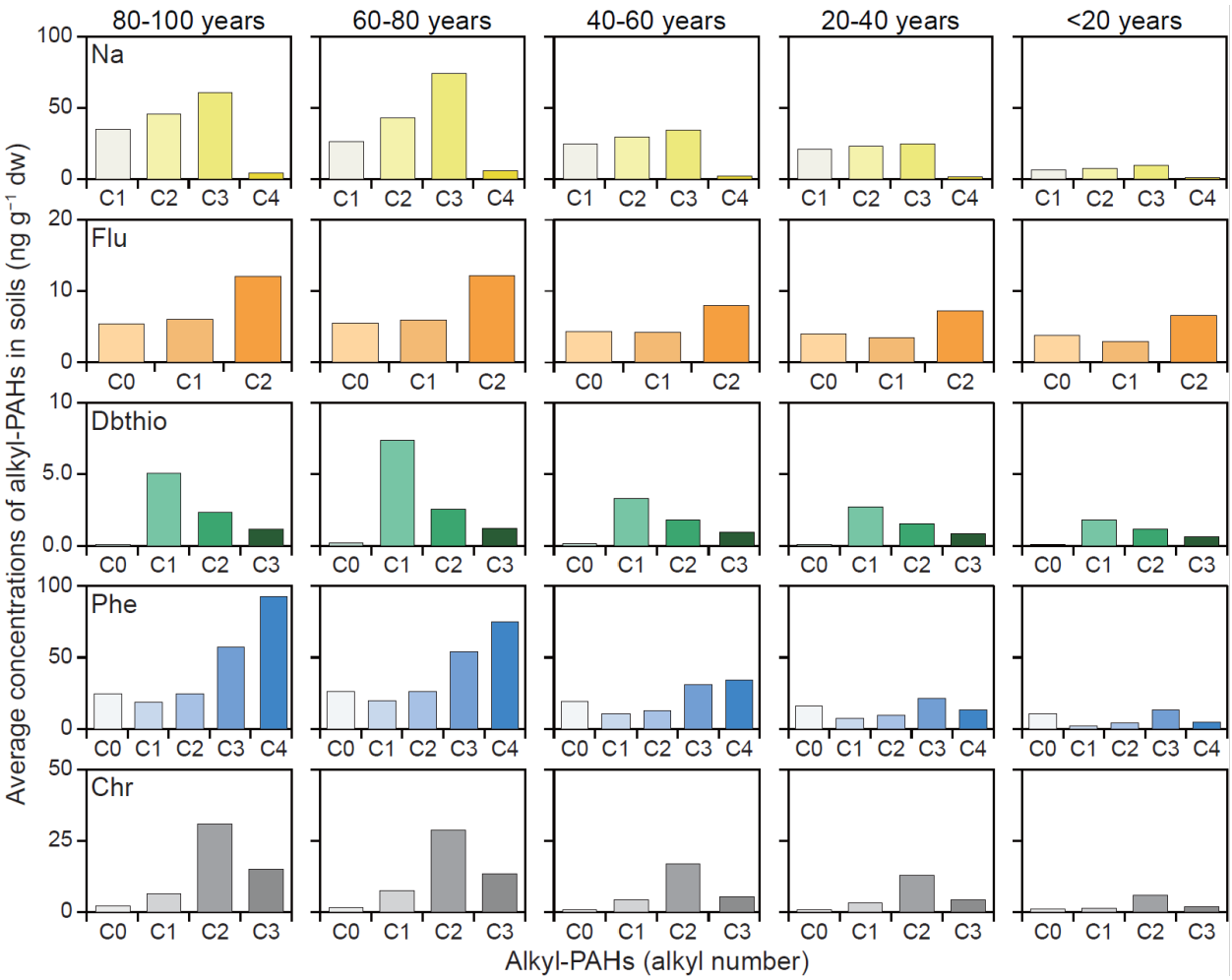

Fig. S7. Relative compositions of alkyl-PAHs in soil samples from the glacier foreland of Midtre Lovénbreen, Svalbard.

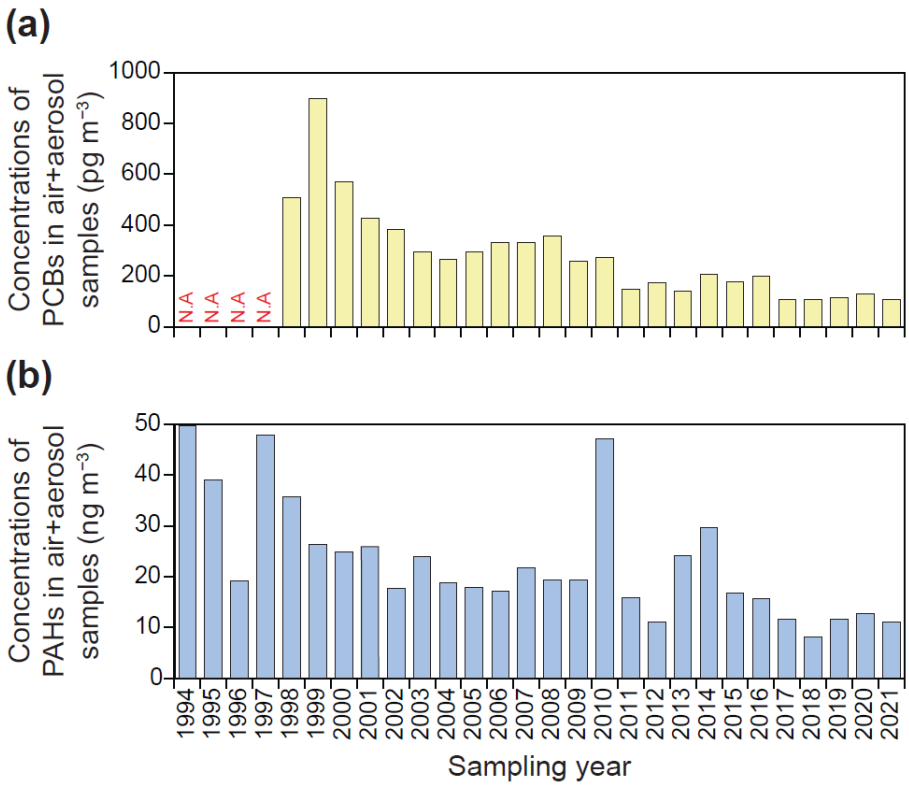

Fig. S8. Concentrations of **(a)** PCBs and **(b)** PAHs in air and aerosol samples measured at the Zeppelin Observatory in the Arctic Svalbard. All data on PCBs and PAHs in the air samples were obtained from the EBAS database of the Norwegian Institute for Air Research (http://ebas.nilu.no/).

References

Brust, G.E., 2019. Chapter 9 - Management Strategies for Organic Vegetable Fertility. In: Biswas, Micallef, editors. Safety and Practice for Organic Food. Academic Press, pp. 193–212. https://doi.org/10.1016/B978-0-12-812060-6.00009-X.

Førland, E.J., Benestad, R., Hanssen-Bauer, I., Haugen, J.E., Skaugen, T.E., 2011. Temperature and precipitation development at Svalbard 1900–2100. Adv. Meteorol. 2011, 893790. https://doi.org/10.1155/2011/893790.

Kim, Y.J., Laffly, D., Kim, S.-e., Nilsen, L., Chi, J., Nam, S., Lee, Y.B., Jeong, S., Mishra, U., Lee, Y.K., Jung, J.Y., 2022. Chronological changes in soil biogeochemical properties of the glacier foreland of Midtre Lovénbreen, Svalbard, attributed to soil-forming factors. Geoderma 415, 115777. https://doi.org/10.1016/j.geoderma.2022.115777.

Leirós, M.C., Trasar-Cepeda, C., Seoane, S., Gil-Sotres, F., 1999. Dependence of mineralization of soil organic matter on temperature and moisture. Soil Biol. Biochem. 31, 327–335. https://doi.org/10.1016/S0038-0717(98)00129-1.

Pessi, I.S., Pushkareva, E., Lara, Y., Borderie, F., Wilmotte, A., Elster, J., 2019. Marked Succession of Cyanobacterial Communities Following Glacier Retreat in the High Arctic. Microb. Ecol. 77, 136–147. https://doi.org/10.1007/s00248-018-1203-3.

Wietrzyk, P., Rola, K., Osyczka, P., Nicia, P., Szymański, W., Węgrzyn, M., 2018. The relationships between soil chemical properties and vegetation succession in the aspect of changes of distance from the glacier forehead and time elapsed after glacier retreat in the Irenebreen foreland (NW Svalbard). Plant Soil 428, 195–211. https://doi.org/10.1017/s11104-018-3660-03.